



**Tiago Novello de Brito**

## **Discrete Line Fields on Surfaces**

### **Tese de Doutorado**

Thesis presented to the Programa de Pós-Graduação em Matemática of PUC-Rio in partial fulfillment of the requirements for the degree of Doutor em Matemática.

Advisor : Prof. Carlos Tomei  
Co-advisor: Prof. João Antônio Recio da Paixão

Rio de Janeiro  
September 2018



**Tiago Novello de Brito**

## **Discrete Line Fields on Surfaces**

Thesis presented to the Programa de Pós-Graduação em Matemática of PUC-Rio in partial fulfillment of the requirements for the degree of Doutor em Matemática. Approved by the undersigned Examination Committee.

**Prof. Carlos Tomei**

Advisor

Departamento de Matemática – PUC-Rio

**Prof. João Antônio Recio da Paixão**

Co-advisor

Instituto de Matemática – UFRJ

**Prof. Thomas Maurice Lewiner**

The Boston Consulting Group

**Prof. Bruno Benedetti**

University of Miami

**Prof. Dimas Martínez Morera**

Departamento de Matemática – UFAM

**Prof. Antonio Castelo Filho**

Instituto de Ciências Matemáticas e de Computação – USP

**Prof. Luiz Henrique de Figueiredo**

Instituto de Matemática Pura e Aplicada – IMPA

**Prof. Marcos Craizer**

Departamento de Matemática – PUC-Rio

**Prof. Márcio da Silveira Carvalho**

Vice Dean of Graduate Studies

Centro Técnico Científico – PUC-Rio

Rio de Janeiro, September 26th, 2018

All rights reserved.

### **Tiago Novello de Brito**

Tiago Novello received his Licenciature degree in Mathematics from Universidade Estadual do Paraná (UNESPAR) in 2012. In 2014, he obtained a Master of Science degree in Mathematics at Universidade Federal de Alagoas (UFAL) under the supervision of Thales Vieira and Dimas Martinez with focus in Computer Graphics. During his doctorate at PUC-Rio, he also studied at the University of Miami under the guidance of Bruno Benedetti. His interests include computational topology, computational geometry, discrete Morse theory, and discrete differential geometry.

#### Bibliographic data

Novello de Brito, Tiago

Discrete Line Fields on Surfaces / Tiago Novello de Brito; advisor: Carlos Tomei; co-advisor: João Antônio Recio da Paixão. – Rio de Janeiro: PUC-Rio, Departamento de Matemática, 2018.

v., 56 f: il. color. ; 30 cm

Tese (doutorado) - Pontifícia Universidade Católica do Rio de Janeiro, Departamento de Matemática.

Inclui referências bibliográficas.

1. Matemática – Teses. 2. Campos de vetores. 3. Campos de linhas. 4. Campos de vetores discretos. 5. Campos de linhas discretos. 6. Decomposição de Morse–Smale. I. Tomei, Carlos. II. Paixão, João Antônio Recio da. III. Pontifícia Universidade Católica do Rio de Janeiro. Departamento de Matemática. IV. Título.

CDD: 510

## Acknowledgements

I would like to express my sincere gratitude to my advisers: João Paixão, for the trust, dedication, and genuine friendship, to whom I will be eternally grateful; Thomas Lewiner, for believing and trusting in my work; Carlos Tomei, for the valuable teachings. To them, my infinite respect and friendship.

I wish to offer my thanks to the Departamento de Matemática of PUC-Rio and its professors for helping me to be a better professional. In particular, Creuza, Kátia, and Orlando, who have always been very efficient and helpful.

I also would like to thank my friends at PUC-Rio, without which this thesis would not have been completed: Armando, Adrian, Renata, Cabral, Jyrko, Alessandro, Gabrielle, Dania, Fernando, Marcelo, Leticia, Cléa, Tamires, Makson, Renan, and so many others.

I thank my parents Clarinda and José Carlos and my brother Rafael for their constant support and care. I am also grateful to Laice Alves for the affection and patience, even in difficult times.

This study was financed in part by the Coordenação de Aperfeiçoamento de Pessoal de Nível Superior - Brasil (CAPES) - Finance Code 001.



## Abstract

Novello de Brito, Tiago; Tomei, Carlos (Advisor); Paixão, João Antônio Recio da (Co-Advisor). **Discrete Line Fields on Surfaces**. Rio de Janeiro, 2018. 56p. Tese de Doutorado – Departamento de Matemática, Pontifícia Universidade Católica do Rio de Janeiro.

A line field on a surface is a smooth map that assigns a tangent line to all but a finite number of points. Such fields model a number of geometric and physical properties, e.g. the principal curvature directions on surfaces or the stress flux in elasticity. They can be seen as a generalization of vector fields. To understand a line field, it is common to study the behavior of its orbits, which can have many different patterns. To this end, we consider a topological approach: we use the critical points and separatrices to decompose the field in regions of similar behavior. We focus on fields that have a Morse–Smale structure. This allows operations like the cancellation of critical points controlled directly in the field decomposition, which is essential for noise removal (topology simplification) on fields coming from simulations or sampling of real-world problems. Based on the decomposition of a Morse–Smale vector field and on cancellation of critical points, Robin Forman introduced a discrete definition for Morse–Smale vector fields. This thesis provides a purely combinatorial definition of line fields, the discrete line fields, entailing Forman’s discrete constructions for vector fields through a new representation of these. Discrete line fields admit a (Morse–Smale type of) decomposition that generates a bridge between discrete and smooth line fields, thus guaranteeing the topological consistency of the definition. We also use double branched coverings to suspend discrete line fields to discrete vector fields, so that vector field tools can be used for discrete line fields. Finally we provide, for a discrete line field, a topologically consistent (Morse-like) cancellation of critical elements. This allows a simplification of the discrete line field topology retaining only the most significant features.

## Keywords

Vector fields; Line fields; Discrete vector fields; Discrete line fields; Morse–Smale decomposition.

## Resumo

Novello de Brito, Tiago; Tomei, Carlos; Paixão, João Antônio Recio da. **Campos de Linhas Discretos sobre Superfícies**. Rio de Janeiro, 2018. 56p. Tese de Doutorado – Departamento de Matemática, Pontifícia Universidade Católica do Rio de Janeiro.

Um campo de linhas sobre uma superfície é um mapa suave que atribui uma linha tangente a todos, exceto a um número finito de pontos. Esses campos modelam um número de propriedades geométricas e físicas, tais como as direções de curvatura principais nas superfícies ou o fluxo de tensão na elasticidade. Para entender um campo de linha, é usual estudar o comportamento de suas órbitas, que podem apresentar diferentes padrões. Para este fim, consideramos uma abordagem topológica que consiste em utilizar os pontos críticos e separatrizes para decompor o campo em regiões de comportamento homogêneo. Focamos em campos que possuem uma estrutura de Morse–Smale. Isso permite operações como o cancelamento de pontos críticos controlados diretamente na decomposição de campo, o que é essencial para a remoção de ruído (simplificação da topologia) em campos provenientes de simulações ou amostragem de problemas do mundo real. Baseado na decomposição de um campo vetorial de Morse–Smale e no cancelamento de pontos críticos, Robin Forman introduziu uma definição discreta para esses campos. O presente trabalho fornece uma definição puramente combinatória para campos de linhas, os campos de linhas discretos, que implicam as construções discretas de Forman para campos de vetores por meio de uma nova representação destes. Campos de linhas discretos admitem uma decomposição que gera uma ponte entre os campos de linhas discretos e suaves, garantindo dessa forma a consistência topológica da definição. Também estabelecemos uma conexão entre um campo de linha discreto e um campo vetorial discreto, desse modo as ferramentas de campos de vetores podem ser usadas em campos de linhas. O trabalho fornece ainda um cancelamento topologicamente consistente de seus elementos críticos para um campo de linha discreto.

## Palavras-chave

Campos de vetores; Campos de linhas; Campos de vetores discretos; Campos de linhas discretos; Decomposição de Morse–Smale.

## Table of contents

1	Introduction	10
2	Basic definitions	13
2.1	Decompositions of a compact surface and rotational systems	13
2.2	Bipartite 4-decomposition	14
3	Vector fields	16
3.1	Smooth vector fields	17
3.2	Discrete vector fields	21
3.2.1	Critical elements and topological properties	25
3.2.2	Smooth vector fields and discrete vector fields	27
3.2.3	Discrete vector fields and Morse matchings	28
4	Line fields	30
4.1	Smooth line fields	30
4.2	Discrete line fields	35
4.2.1	Critical elements and topological properties	38
4.2.2	Smooth line fields and discrete line fields	41
4.2.3	Discrete line fields and Morse matchings	41
4.3	Cancellation in discrete line fields	42
5	From discrete line to discrete vector fields	44
5.1	Discrete vector fields and discrete line fields	44
5.1.1	Orientable discrete line fields	44
5.1.2	Non-orientable discrete line fields: double branched coverings	46
6	Conclusion and future work	49
	Bibliography	51
A	Discrete Morse theory	55

## List of figures

Figure 1.1	(a) a line field, the dots are the critical points of the line field, (b) the critical points and the separatrices decompose the phase space in regions.	10
Figure 2.1	Two decompositions of the sphere: (a) a cube, (b) and (c) equivalent decompositions consisting of two vertices, one edge, and one face.	14
Figure 2.2	(a) the face diagonals of a bipartite 4-decomposition, joining the white dots. (b) the decomposition associated to the face diagonals. (c) and (d) the analogous construction for the face diagonals connecting the black dots.	15
Figure 3.1	(a) a 6-saddle point. (b) and (c) two possible perturbations of (a).	17
Figure 3.2	(a) an unstable orbit. (b), (c) two perturbations (from [14]).	18
Figure 3.3	Peixoto's counterexample for the characterization of topological type of a MS line field through its orgraph. The green cycle represents the meridian of the sphere. (from [17]).	19
Figure 3.4	(a) a MS vector field, (b) the MS decomposition.	20
Figure 3.5	The opposite sides of the squares are identified providing a torus. (a) two critical points joined by a unique edge in a MS vector field. (b) the result of applying Theorem 3.3 to (a).	21
Figure 3.6	The squares represent the surface of the torus. (a) a bipartite 4-decomposition, and in (b) each face of (a) gets a grey point. (c), (d) the bipartite 4-decomposition. (e) the MS vector field correspondent to (d) stated by Theorem 3.2.	22
Figure 3.7	(a) a matching between a vertex and a face diagonal. (b) the resulting bipartite 4-decomposition after cancellation of the matched cells.	24
Figure 3.8	(a) a discrete vector field, the critical cells are in red. (b) the MS decomposition of (a).	27
Figure 3.9	(a) a Morse matching. (b) the overlap of (a) by its bipartite 4-decomposition. (c) the corresponding discrete vector field.	29
Figure 4.1	The list of all structurally stable critical points allowed in a smooth line field. The last four types of critical points are not present in line fields.	31
Figure 4.2	(a) a MS line field with two 3-saddle and three focus points on the sphere. (b) the suspension of the MS line field; white (black) dots represent the minima (maxima).	33
Figure 4.3	(a) the MS decomposition of the triple presented in Figure 4.2(b). (b) the MS decomposition of the line field given in Figure 4.2(a).	33

Figure 4.4	The saddles allowed in generalized MS line fields.	34
Figure 4.5	(a) a decomposition of the sphere into two triangles. (b) each triangle receives a grey point. (c) and (d) the bipartite 4-decomposition.	36
Figure 4.6	(a) a piece of a decomposition. (b) the associated bipartite quadrilateral embedding. (c) the corresponding line field.	36
Figure 4.7	(a) presents a discrete line field with a singleton matching; (b) is the result of applying Lemma 4.5 to (a). Finally, Lemma 4.6 applied to (b) is expressed in (c) and (d).	37
Figure 4.8	(a) a decomposition of the sphere. (c) a discrete line field.	38
Figure 4.9	(a) a discrete line field. (b)-(d) the proof's idea of Theorem 4.8.	39
Figure 4.10	(a) a discrete line field, the critical cells are in red. (b) the MS decomposition of (a).	40
Figure 4.11	(a) and (c) are Figure 3.9. (d) adding a matching between a vertex and edge; (e) the matching on the original decomposition.	42
Figure 4.12	(a) the two critical triangles in red are in the boundary of a unique face of the MS decomposition. (b) the cancellation between the critical faces.	43
Figure 4.13	(a) a critical face and a critical vertex connected by a unique path. (b) the reversed path.	43
Figure 5.1	(a) and (b) present a non-bipartite 4-decomposition of the torus and a bipartite 4-decomposition.	45
Figure 5.2	(a) a hexagon with no matched edge; in (b) a subdivision into two 4-gons. (c) a pentagon with a unique matched edge; (d) a subdivision into a 4-gon and a regular triangle.	45
Figure 5.3	Different colors receive the number 0, and 1 otherwise. (a) the suspension of an edge signed with 1. (b) the suspension of an edge signed with 0. (c) combines (a) and (b).	46
Figure 5.4	The edges assignment is similar to Figure 5.3. (a) a decomposition containing two faces; (b) the derived decomposition.	47
Figure 5.5	(a) a non-orientable discrete line field. (b) the suspension to an orientable field.	47
Figure 6.1	(a) a bitorus. (b) a sample of the minimum curvature vector field over the vertices of a decomposition of the bitorus.	49
Figure A.1	(a) a decomposition. (b) the Hasse diagram. (c) a Morse matching.	55

# 1

## Introduction

A line field on a surface is a smooth map which assigns a tangent line to all but a finite number of points. Such fields model a number of physical properties, like velocity and temperature gradient in fluid flow [1], stress, and momentum flux in elasticity [2]. In computer graphics, line fields are often studied in topological segmentation of fields [3, 4, 5], remeshing [6, 7, 8], and are helpful for the visualization of vector/line/symmetric tensor fields [9, 10, 11, 12, 13, 14, 15].

To analyze a line field, it is common to study the behavior of its orbits [10, 14]. We take a more topological approach, consisting of grouping orbits with similar behavior [16, 17]. To construct such a decomposition, we observe that the dynamics of a line field is usually trivial almost everywhere except near the points for which the field is not defined or vanishes, the so called critical points [18] (Figure 1.1). Such points are usually connected by *separatrices*, which in turn partition the phase space (Figures 1.1(b)). For computations, it is essential that such orbit decomposition be maintained over small perturbations of the field [10, 14]. Such *structurally stable* fields are well studied in the dynamical systems literature [17, 19, 20].

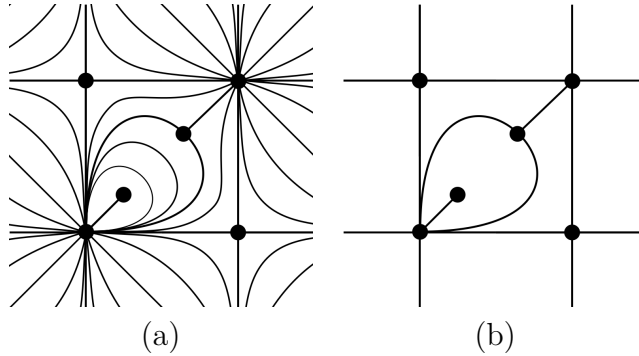


Figure 1.1: (a) a line field, the dots are the critical points of the line field, (b) the critical points and the separatrices decompose the phase space in regions.

In this work we obtain combinatorial descriptions of structurally stable fields. Most ideas are inspired by constructions associated to (continuous) line fields. Restricted to the vector field setting, Andronov and Pontryagin [19] provided a list of combinatorial properties characterizing a structurally stable (smooth) vector field, frequently called a *Morse–Smale* (MS) field.

Peixoto [17] proved that the critical points and separatrices of a MS vector field produce a (MS) decomposition of the underlying surface with no critical points in the interior of each two 2-cell. Additionally, such MS decomposition characterizes the class of topologically equivalent of the MS vector field (Theorem 3.2, a vertical bijection in Diagram 1.1).

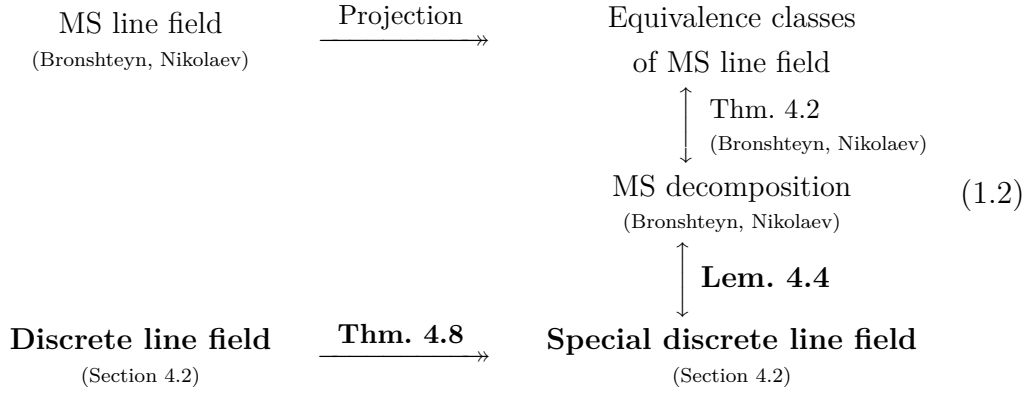
$$\begin{array}{ccc}
 \text{MS vector field} & \xrightarrow{\text{Projection}} & \text{Equivalence classes} \\
 \text{(Andronov and Pontryagin)} & & \text{of MS vector field} \\
 & & \updownarrow \begin{array}{c} \text{Thm. 3.2} \\ \text{(Peixoto)} \end{array} \\
 & & \text{MS decomposition} \\
 & & \text{(Peixoto)} \\
 & & \updownarrow \text{Lem. 3.4} \\
 \text{Discrete vector field} & \xrightarrow[\text{Forman}]{\text{Thm. 3.6}} & \text{Special discrete vector field} \\
 \text{(Forman)} & & 
 \end{array} \tag{1.1}$$

Deformations of vector fields may lead to cancellation of critical points, a technique widely used by Morse [21] yielding substantial simplification of vector fields without altering the topological type of the underlying surface.

Forman [22, 23] proposed a definition of a *discrete (Morse–Smale) vector field*, which is presented for the convenience of the reader in Section 3.2. Morse cancellation takes a privileged place in this context: each discrete vector field gives rise to a special model (in a sense to be specified in Section 3.2) and such models are in one-to-one correspondence with MS decompositions of a (continuous) vector field (Corollary 3.7, the composition of some functions in the diagram). The result follows from Forman’s fundamental characterization of the homotopy type of the underlying decomposition of a discrete vector field in terms of its critical cells (Theorem 3.6).

One of the algorithmic upshots of Forman theory is the construction of a (Morse–Smale type of) decomposition through the definition of (discrete) critical elements and orbits (paths). This decomposition represent the standard MS decomposition of a MS vector field which allows for simpler combinatorial operations: as a (Morse-like) cancellation of critical elements.

The analogous result of Theorem 3.2 for line fields, Theorem 4.2, was introduced by Bronshteyn and Nikolaev [24, 25]: they defined MS line fields, showed their structural stability and presented their MS decomposition. In this thesis, we extend Forman’s theory to line fields, the bottom line of Diagram 1.2.



Forman's discrete vector fields are special cases of such *discrete line fields*, as smooth vector fields are special cases of line fields. The first step towards the new definition consists of a representation of a Forman's vector field by means of *bipartite 4-decompositions* (also called *radial graphs* [26, 27, 28]). Dropping some of the properties of such discretization then yields the desired definition.

As in Forman's theory, our definition provides an Euler–Poincaré formula (Theorem 4.7), and a homotopy theorem (Theorem 4.8 in analogy to Theorem 3.6) which again induces a bijection between MS decomposition and equivalence classes of homotopical MS line fields. Such MS decomposition partition the discrete line field in regions with no critical elements.

**Theorem (Homotopy)** *The underlying decomposition of a discrete line field is homotopy equivalent to a decomposition consisting only of its critical cells.*

Inspired by Morse's cancellation of critical points in a MS vector field, we propose two consistent cancellations of critical elements in a discrete line field (Propositions 4.10 and 4.11), which entail Forman's cancellation of critical elements [23], widely used in applications [4, 29, 30, 31].

**Theorem (Cancellation)** *Two critical elements in a discrete line field can be merged if there is a unique path connection between them.*

We now consider a different issue. Following ideas dating back to the theory of Riemann surfaces, Bronshteyn and Nikolaev [16] studied a MS line field by considering a suspension of such field to a vector field on a double branched covering. Branch points are the non-orientable critical points. Such construction bridges continuous line and vector fields, and allows for transferring results and algorithms between contexts. We propose a discrete version: a discrete line field suspends to a discrete vector field.

**Theorem (Suspension)** *Every discrete line field can be suspended to a discrete vector field, on a double branched covering of their underlying surfaces. The branched points belong to the non-oriented critical elements.*



## 2

### Basic definitions

We use extensively some special (CW) decompositions of a compact surface, following the standard notation from Gross and Tucker [32]. Thus, MS decompositions of vector and line fields [16, 17], and discrete vector and line fields depend of such decompositions.

A special case, the bipartite 4-decomposition [26, 28], is used in Chapter 3 to provide an alternative definition of Forman's concept of discrete vector field [23] and in the MS decompositions of discrete vector and line fields.

#### 2.1

##### Decompositions of a compact surface and rotational systems

In this section we present two equivalent discrete representations of a compact (orientable) surface: 2-cell embeddings and rotational systems.

We follow the notation of Gross and Tucker [32]. Let  $S$  be a connected compact surface. An *embedding*  $i : G \rightarrow S$  of a finite graph  $G$  into  $S$  is an injective continuous map. Two embeddings  $i_1$  and  $i_2$  of  $G$  in  $S$  are *equivalent* if there is a homeomorphism  $h : S \rightarrow S$  such that  $h \circ i_1 = i_2$ . In a *2-cell embedding*  $i : G \rightarrow S$ , the components of the set  $S \setminus i(G)$ , the 2-cells, are homeomorphic to open discs. A 2-cell embedding  $i : G \rightarrow S$  induces a (CW) *decomposition*  $\mathcal{S} = (V, E, F)$  of  $S$ , where  $i(G) = (V, E)$  is obtained as follows. The set of vertices  $V$  and the set of edges  $E$  are the images of the elements of  $G$ , and the set of faces  $F$  is the set of 2-cells of  $S \setminus i(G)$  (Figure 2.1).

We frequently need notation for the boundary of a face  $f$ . We list edges and vertices along the boundary cyclically, inducing the *boundary walk*  $v_1 e_1 v_2 e_2 \dots v_k e_k v_{k+1}$ , with  $v_{k+1} = v_1$ . Here, for  $i = 1 \dots k$ , the edge  $e_i$  runs from  $v_i$  to  $v_{i+1}$ . Thus  $f$ , up to homeomorphism, is a *k-gon*, i.e., a  $k$ -regular polygon with identifications on its edges. In Figure 2.1(a), a simple decomposition of the sphere, the faces are 4-gons. Figure 2.1(b) is an extreme case, in which the sphere is obtained from a single 2-gon. This rather peculiar example will be used sometimes as a special case.

Stahl [33] described another representation for the decomposition  $\mathcal{S} = (V, E, F)$  of a compact, oriented surface  $S$ . Draw a (topological) circle around a vertex  $v$  and orient it positively with respect to the orientation of  $S$ . The

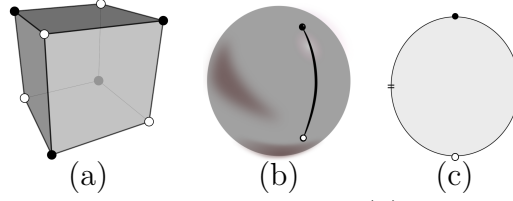


Figure 2.1: Two decompositions of the sphere: (a) a cube, (b) and (c) equivalent decompositions consisting of two vertices, one edge, and one face.

circle intersects the edges incident at  $v$  at a set of points with a cyclic order. The set of all such ordered cycles, one per vertex, is a *rotational system*  $\mathcal{R}$ .

We now invert the procedure. A *rotational system*  $\mathcal{R}$  on a finite graph  $G = (V, E)$  consists of a choice of a cyclic ordering on each set of edges with a common vertex. Two graphs  $G_1$  and  $G_2$  endowed with rotational systems  $\mathcal{R}_1$  and  $\mathcal{R}_2$  are *equivalent* if there is a graph isomorphism from  $G_1$  to  $G_2$ , which either preserves or reverses all of the cyclic orderings induced by  $\mathcal{R}_1$  and  $\mathcal{R}_2$ . It turns out that  $G$  and  $\mathcal{R}$  suffice to describe a surface  $S$ .

**Theorem 2.1 (Stahl [33])** *Every rotational system  $\mathcal{R}$  on a finite graph  $G = (V, E)$  induces a 2-cell embedding in an oriented surface  $S$  with a decomposition  $\mathcal{S} = (V, E, F)$ . All such embeddings of  $G$  are equivalent.*

Algorithm 1 [32] explicitly reconstructs the decomposition associated to a graph endowed with a rotational system, as stated in Theorem 2.1.

**Data:** A graph  $G = (V, E)$  and a rotational system  $\mathcal{R}$ .

**Result:** Decomposition  $\mathcal{S} = (V, E, F)$  of a compact surface  $S$ .

```

while There is an edge  $e = [u, w]$  adjacent to less than two faces in  $F$  do
    take the order that reverses any existing boundary walk containing  $e$ ;
    create an empty face  $f$ ;
    while  $w \neq u$  do
        add  $e$  to the boundary walk of  $f$  ;
        update  $e$  by  $\mathcal{R}$  to the next edge  $[w, u']$  in  $w$ ;
        replace  $w$  by  $u'$ ;
    end
    add  $f$  to  $F$ .
end

```

**Algorithm 1:** Face Tracing Algorithm [32].

## 2.2

### Bipartite 4-decomposition

We define Pisanski's *bipartite 4-decomposition* of compact surfaces [28]. Bipartite 4-decompositions are in correspondence with decompositions of compact surfaces [27, 28]. Also, as we will see in Chapter 3, the MS decompositions of MS vector fields correspond to bipartite 4-decompositions [16, 17].

A decomposition  $\mathcal{S} = (V, E, F)$  of  $S$  is called a *4-decomposition* if the set of faces  $F$  consists of either only 4-gons (as Figure 2.1(a)) or a single 2-gon (as

Figure 2.1(b)), the latter being a special case. When the graph  $G$  is bipartite<sup>1</sup>,  $\mathcal{S}$  is called a *bipartite 4-decomposition*. Figure 2.1 provides two examples.

The notion of a bipartite 4-decomposition of a compact surface  $S$  may seem restricted. However, Pisanski and Malnič [28] provided a construction of a bipartite 4-decomposition of  $S$  from any 2-cell decomposition of  $S$ .

For a decomposition  $\mathcal{S} = (V, E, F)$  of a compact surface  $S$ , we define a bipartite graph  $G = (V_G, E_G)$  as follows.  $V_G$  is the union of  $V$  and a point in the interior of each face of  $\mathcal{S}$ . The edges  $E_G$  indicate the adjacency relations between vertices and faces, and they are represented by disjoint arcs in  $S$ . The graph  $G$  is bipartite and naturally embedded in  $S$  and produces a 4-decomposition  $\mathcal{S}$ . This object is called a *bipartite 4-decomposition* of  $\mathcal{S}$  and denoted as  $\mathcal{M}(\mathcal{S})$ . For instance, Figure 2.2(a) provides a bipartite 4-decomposition of Figure 2.2(b).

The embedding associated to the bipartite 4-decomposition  $\mathcal{M}(\mathcal{S})$  of  $\mathcal{S}$  is known in the literature as the *radial graph* of  $\mathcal{S}$  [26, 28]. The following result is a characterization of bipartite 4-decompositions.

**Theorem 2.2 (Pisanski–Malnič[28])** *Let  $\mathcal{M}$  be a bipartite 4-decomposition of the surface  $S$ . Then, up to equivalence, there are only two decompositions  $\mathcal{S}_1$  and  $\mathcal{S}_2$  of  $S$  whose bipartite 4-decompositions  $\mathcal{M}(\mathcal{S}_i)$  are equivalent to  $\mathcal{M}$ .*

The decompositions in the statement are obtained as follows: for  $G = (V, E)$ , we split  $V$  into two disjoint sets,  $V_1$  and  $V_2$ , since  $G$  is bipartite. We construct the decomposition  $\mathcal{S}_1$  such that its set of vertices is  $V_1$ . Edges are the face diagonals joining two vertices in  $V_1$ . Finally, faces are components of  $S \setminus (V_1 \cup E)$ , and are identified with the vertices in  $V_2$  (Figures 2.2(a) and (b)). Similarly,  $\mathcal{S}_2$  is built by replacing  $V_1$  by  $V_2$  in the construction of  $\mathcal{S}_1$ . Informally, the chosen face diagonals are “flipped” in the construction of  $\mathcal{S}_1$  (Figure 2.2(c) and (d)). The decomposition  $\mathcal{S}_2$  is called the *dual* of  $\mathcal{S}_1$ . The decomposition  $\mathcal{S}_2$  is often denoted by  $\mathcal{S}_1^*$ .

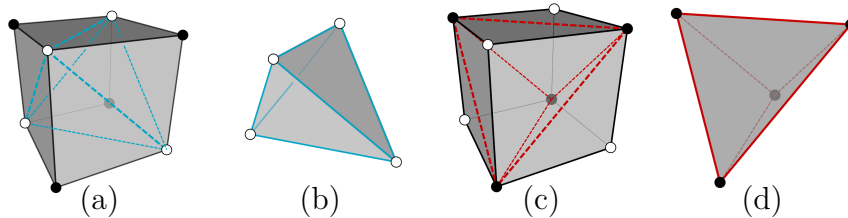


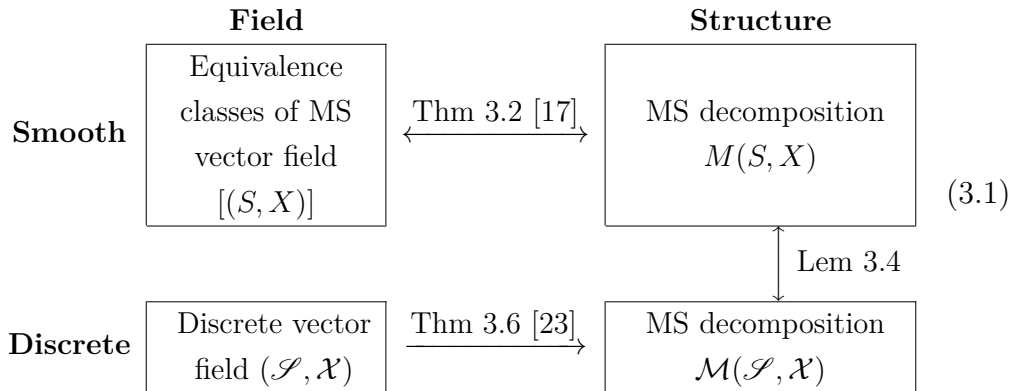
Figure 2.2: (a) the face diagonals of a bipartite 4-decomposition, joining the white dots. (b) the decomposition associated to the face diagonals. (c) and (d) the analogous construction for the face diagonals connecting the black dots.

<sup>1</sup>A graph is bipartite if its vertices can be partitioned into two different sets and no edge is allowed between vertices of a same set.

### 3

## Vector fields

This chapter presents the definitions and main results on MS vector and discrete vector fields. We follow Diagram 3.1, from Chapter 1.



The chapter has two sections. In the first, we define a MS vector field  $(S, X)$  (upper left box of Diagram 3.1) on a compact surface  $S$ , and we construct its MS decomposition  $M(S, X)$  [17]. We finish the section with a correspondence between the equivalence class of  $(S, X)$  and  $M(S, X)$  (Theorem 3.2). The second section presents the analogous discrete concepts of a MS vector field [23], and Theorem 3.6[23]. Lemma 3.4 is a bijection between the MS decompositions of smooth and discrete vector fields.

Corollary 3.7 concludes this chapter by combining the correspondences above to finally show the correspondence between MS vector fields and discrete vector fields [23].

The contribution in this chapter is a new representation of Forman's discrete vector fields (Appendix A) by means of bipartite 4-decompositions, which we will call simply discrete vector fields. This will permit a natural generalization to line fields (Chapter 4) by dropping the bipartite and the 4-decomposition requirements. Because of such generalization, the proofs in this chapter will be given in Chapter 4 in a more general context.

### 3.1

#### Smooth vector fields

Let  $S$  be a compact (possibly orientable) surface and its *tangent bundle*, which is the disjoint union  $TS = \bigsqcup_{p \in S} T_p S$  of its tangent planes  $T_p S$ . We write each element of  $TS$  as a pair  $(p, v)$ , where  $p \in S$  and  $v \in T_p S$ . The map  $\pi : T \rightarrow S$ ,  $\pi(p, v) = p$  is called the *projection map*. A *vector field* is a pair  $(S, X)$ , where  $X : S \rightarrow TS$  is a smooth map satisfying  $\pi \circ X = Id$ .

A point  $p$  in a vector field  $(S, X)$  is said to be *critical* if  $X(p) = (p, 0)$ . A curve  $\gamma : (a, b) \rightarrow S$ , with  $a < b$ , is called an *integral line* of  $(S, X)$  if  $\gamma'(t) = X(\gamma(t))$  for  $t \in (a, b)$ . The integral line  $\gamma$  is an *orbit* of  $(S, X)$  if it is a maximal integral line: there is no other integral line  $\alpha : (c, d) \rightarrow S$ , with  $c < d$ , satisfying  $\gamma(a, b) \subset \alpha(c, d)$ . The field  $(S, X)$  is called *acyclic* when it does not admit a orbit which is a closed curve. We say that two fields  $(S, X_0)$  and  $(S, X_1)$  are *topologically equivalent* if there is a homeomorphism  $h : S \rightarrow S$  mapping orbits from  $(S, X_0)$  to orbits of  $(S, X_1)$ . The equivalence class of  $(S, X_1)$  is denoted by  $[(S, X_1)]$ . We endow the space of smooth vector fields with the uniform  $C^r$ -topology,  $r \geq 1$ .

#### MS vector fields

A vector field  $(S, X)$  is said to be *structurally stable* if it admits an open neighborhood in the space of smooth vector fields consisting of topologically equivalent vector fields. These fields are essential in applications [10, 34].

Consider for example the following *non-stable* situation [10, 34]: a 6-saddle point, that is, a critical point with 6 separatrices (also known as a *monkey saddle*, Figure 3.1(a)). Small perturbations might deform the field into two 4-saddle points (Figure 3.1(b) and (c)).

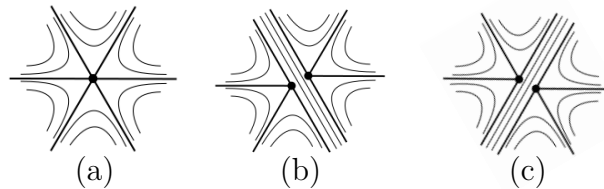


Figure 3.1: (a) a 6-saddle point. (b) and (c) two possible perturbations of (a).

Another frequent situation is the presence of unstable orbits between saddle points (Figure 3.2(a)). Consider the perturbation in Figures 3.2(b) and (c). The critical points in this example are from the context of *line fields* (Section 4.1).

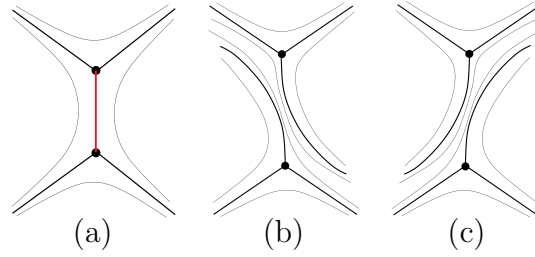


Figure 3.2: (a) an unstable orbit. (b), (c) two perturbations (from [14]).

Andronov and Pontryagin [19] proved that those are the issues to avoid for a vector field to be structurally stable, defining thus the following set of simple geometric properties for an (acyclic) vector field  $(S, X)$ .

- i) There are finitely many critical points, which are necessarily maxima, minima, and 4-saddle points;
- ii) There is no orbits between saddle points;
- iii) The limit sets of each orbit are critical points (there are no closed orbits).

Fields satisfying these properties are called *Morse–Smale* (MS). Peixoto [35] proved that the MS properties are also sufficient for the structural stability of a vector field.

**Theorem 3.1 (Andronov–Pontryagin–Peixoto[19, 35])** *Structurally stable vector fields are in bijection with MS vector fields. Further, they form an open and dense subset of the space of smooth vector fields.*

The second part of Theorem 3.1 states, informally, that every vector field is arbitrarily near a MS vector field. This result is not used in this work, but provides that MS vector fields are robust and abundant.

### MS decomposition

As is well known [32], surfaces admit CW decompositions, which are especially simple in low dimensions. In Section 2.1, we present the standard notation used in this case, following Gross and Tucker [32], and introduce an alternative description of such a decomposition due to Stahl in terms of rotational systems.

Theorem 3.1 opens the door for a combinatorial description of structurally stable vector fields [17], since it gives a correspondence between such fields and MS vector fields. These admit finitely many critical points (Property i) connected by *separatrices*: the orbits which have a 4-saddle point as

limit set (Properties **ii** and **iii**). This suggests the representation of a MS vector field  $(S, X)$  by an *orgraph* (graph of orbits)  $M = (V, E)$ , where the set of vertices  $V$  consists of the critical points of  $(S, X)$  and the edges  $E$  are given by the separatrices between them. The orgraph  $M$  is tripartite<sup>1</sup> by three different sets, the minima (lower level), 4-saddle points (middle level), and maxima (upper level).

Peixoto [17] tried to describe classes of topologically equivalent MS vector fields  $(S, X)$  by the orgraph  $M$ . There is a difficulty, however, presented in Figure 3.3: two isomorphic, abstractly given, orgraphs yielding non-equivalent decompositions of the sphere. Thus, non-equivalent MS vector fields may have isomorphic orgraphs. To overcome this obstruction, a rotational system  $\mathcal{R}$  compatible with the orientation of the underlying surface was required. The motivation behind such a requirement is that any decomposition of a compact surface is completely determined by a graph endowed with a rotational system, as described in Section 2.1.

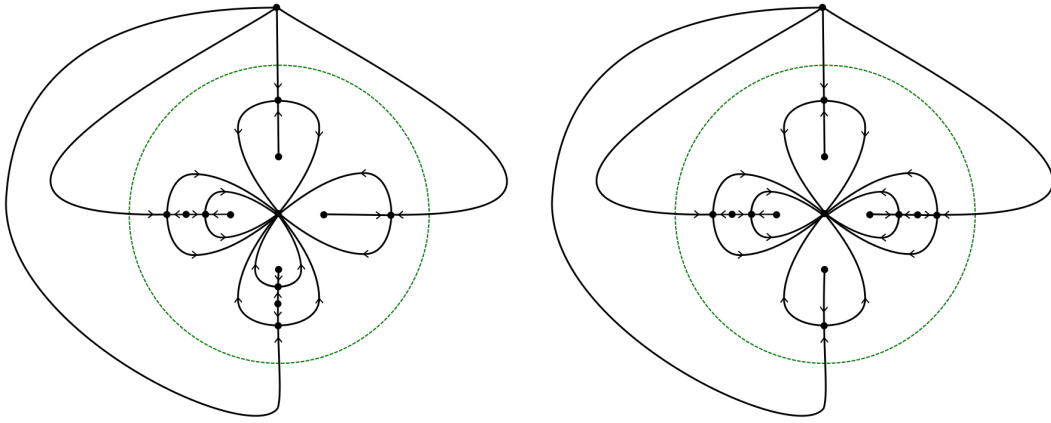


Figure 3.3: Peixoto's counterexample for the characterization of topological type of a MS line field through its orgraph. The green cycle represents the meridian of the sphere. (from [17]).

Theorem 2.1 applied to both the orgraph  $M = (V, E)$  and to the rotational system  $\mathcal{R}$  produces a decomposition  $(V, E, F)$  of  $S$ , which is called the *MS decomposition* of  $(S, X)$  and denoted by  $M(S, X)$ . This decomposition satisfies the following important properties.

- a) The orgraph  $M$  is tripartite (and triangle-free) by three different sets, the minima (lower level), 4-saddles (middle level), and maxima (upper level) of  $(S, X)$ ;
- b) The faces in  $F$  are 4-gons;

<sup>1</sup>A graph is tripartite if its vertices can be partitioned into three different sets and no edge is allowed between vertices of a same set.

- c) The vertices in the middle level have two adjacencies with the upper level and two with the lower level;
- d) If the middle level is empty, then  $M(S, X)$  is a decomposition of the sphere consisting of a unique 2-gon (as in Figure 2.1(b)).

An argument for **b** depends on Property **ii** to be proved in Lemma 4.4, Chapter 4 in a more general context; the other properties follow directly from the MS properties **i** - **iii**. Clearly,  $M(S, X)$  is a bipartite 4-decomposition (Section 2.2), since it is tripartite and triangle-free by Property **a**, thus bipartite, and its faces  $S \setminus M$  are 4-gons by Property **b** (Figures 3.4). A decomposition satisfying Properties **a** - **d** is called an *abstract MS decomposition*.

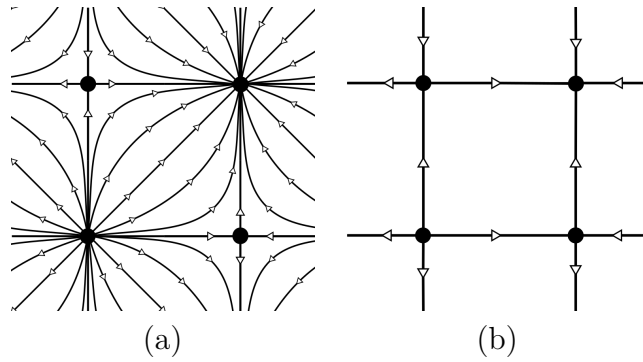


Figure 3.4: (a) a MS vector field, (b) the MS decomposition.

**Theorem 3.2 (Peixoto [17])** *Two MS vector fields are topologically equivalent if and only if their MS decompositions are equivalent. Moreover, every abstract MS decomposition is equivalent to a MS decomposition of a MS vector field.*

$$\begin{array}{ccc} \text{MS vector field} & \xleftrightarrow{\text{Thm 3.2 [17]}} & \text{MS decomposition} \\ [(S, X)] & & M(S, X) \end{array} \quad (3.2)$$

Diagram 3.2 is part of Diagram 3.1 provided in the beginning of this chapter.

### Cancellation of critical points

As Theorem 3.2 provides a discretization of a MS vector field in terms of its MS decomposition, the question now becomes: are there operations in the MS decomposition which reduces the critical points of its MS vector field? Many applications rely on this question, such as reducing the number of critical points in the topological analysis of vector fields [10, 3, 29, 14, 30].

We recall Morse's procedure to cancel critical points of vector fields [21], exemplified in Figure 3.5. Take two critical points connected by a unique



separatrix: the procedure obliterates the separatrix and two critical points and naturally acts on the MS decomposition of the vector field.

**Theorem 3.3 (Morse [21])** *Let  $(S, X)$  be a MS vector field and  $p$  and  $q$  be critical points connected by a unique edge  $e$  in  $M(S, X)$ . Then it is possible to alter the vector field  $(S, X)$  in a small neighborhood  $U$  of  $e$  such that the new field has no critical points in  $U$ .*

Theorem 3.3 states that a pair of critical points connected by a unique edge (as Figure 3.5(a)) in the MS decomposition of a MS vector field provides the cancellation of such points (as Figure 3.5(b)). This motivates Forman's definition of discrete vector fields in the next section.

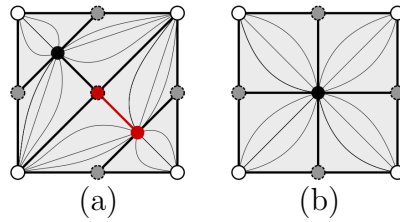


Figure 3.5: The opposite sides of the squares are identified providing a torus. (a) two critical points joined by a unique edge in a MS vector field. (b) the result of applying Theorem 3.3 to (a).

### 3.2

#### Discrete vector fields

In this section we reinterpret Forman's Morse matching [23], presented in Appendix A. We replace a smooth (acyclic) vector field  $(S, X)$  on a compact surface  $S$  by a pair  $(\mathcal{S}, \mathcal{X})$ , called *discrete (acyclic) vector field*, which consists of a bipartite 4-decomposition  $\mathcal{S}$  of  $S$ , and a matching  $\mathcal{X}$  between vertices and adjacent face's diagonals. We provide an alternative representation of a discrete vector field  $(\mathcal{S}, \mathcal{X})$  by an inductive approach.

#### Discrete vector fields with empty matching

To analyze a discrete vector field  $(\mathcal{S}, \emptyset)$ , take  $\mathcal{S} = (V, E, F)$  as a bipartite 4-decomposition of a compact surface  $S$  (for the definition and basic properties, see Section 2.2). The set of vertices  $V$  admits a bipartition  $W \sqcup B$  and  $S \setminus (V, E)$  consists of 4-gons. We call the vertices in  $W$  and  $B$  *white* and *black*. Now, let  $\mathcal{M}(\mathcal{S}, \emptyset)$  be the bipartite 4-decomposition of  $\mathcal{S}$ , as stated in Theorem 2.2. This object, naturally, enjoys the following properties:

- a) The vertices and edges of  $\mathcal{M}(\mathcal{S}, \emptyset)$  induces a tripartite (and triangle-free) by three different sets, the white vertices (lower level), the 4-gons (middle level), and the black vertices (upper level);
- b) The faces of  $\mathcal{M}(\mathcal{S}, \emptyset)$  are 4-gons;
- c) The vertices in the middle level have two adjacencies with the upper level and two adjacencies with the lower level;
- d) If the middle level is empty, then  $\mathcal{M}(\mathcal{S}, \emptyset)$  is a decomposition of the sphere consisting of two vertices connected by an edge (special case).

The decomposition  $\mathcal{M}(\mathcal{S}, \emptyset)$  is called the *MS decomposition* of  $(\mathcal{S}, \emptyset)$  (Figures 3.6(a)-(d)). Properties **a** - **d** are identical to Properties **a** - **d** of the MS decomposition of a MS vector field. The next lemma states this correspondence.

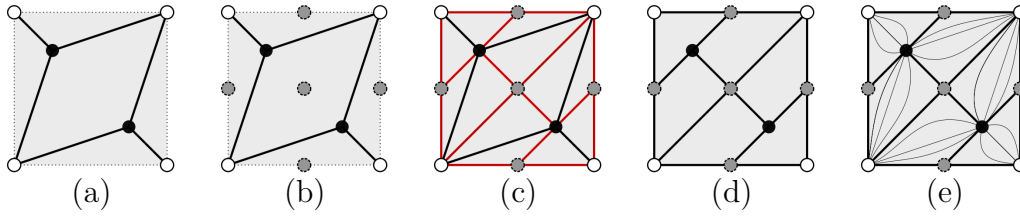


Figure 3.6: The squares represent the surface of the torus. (a) a bipartite 4-decomposition, and in (b) each face of (a) gets a grey point. (c), (d) the bipartite 4-decomposition. (e) the MS vector field correspondent to (d) stated by Theorem 3.2.

**Lemma 3.4** *The MS decomposition  $\mathcal{M}(\mathcal{S}, \emptyset)$  of a discrete vector field  $(\mathcal{S}, \emptyset)$  is equivalent to a MS decomposition  $M(S, X)$  of a MS vector field  $(S, X)$ .*

$$\begin{array}{ccc} \text{MS decomposition} & \xleftrightarrow{\text{Lemma 3.4}} & \text{MS decomposition} \\ \mathcal{M}(\mathcal{S}, \emptyset) & & M(S, X) \end{array} \quad (3.3)$$

Lemma 3.4 ensures that the minima, maxima, and 4-saddles in a MS vector field correspond to the white vertices, black vertices, and 4-gons, respectively, in a discrete vector field  $(\mathcal{S}, \emptyset)$  (Figure 3.6).

If the reader is familiar with Morse matchings, the following connection may be interesting. Observe that Theorem 2.2 applied to the bipartite 4-decomposition  $\mathcal{S}$  returns a decomposition  $\mathcal{S}_1$ , for which its vertices, faces, and edges (critical elements of an empty Morse matching) correspond to the white vertices, black vertices, and faces of  $\mathcal{S}$ , respectively (Table 3.1).

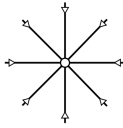

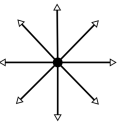
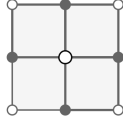
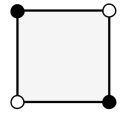
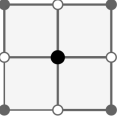
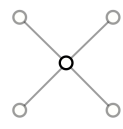
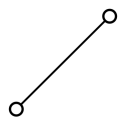
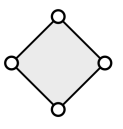
	Minimum	4-saddle	Maximum
MS vector field			
Discrete vector field	 white vertex	 4-gon	 black vertex
Morse matching (Forman's discrete vector field)	 vertex	 edge	 face

Table 3.1: Diagram among critical elements of MS vector fields, discrete vector fields, and Morse matchings.

### The singleton matching

We now introduce a discrete vector field  $(\mathcal{S}, \mathcal{X})$  with a singleton matching, where  $|\mathcal{X}| = 1$ . This matching is motivated by Morse cancellation (Theorem 3.3) of critical points. Let  $p$  and  $q$  be two critical points in a MS vector field  $(S, X)$  connected by a unique separatrix (Figure 3.5(a)). Either  $p$  or  $q$  must be a 4-saddle since Property **ii** of a MS vector field says that there is no orbits between 4-saddle points. Without loss of generality we assume that  $p$  is the 4-saddle point. Then,  $q$  is either a minimum or a maximum. The first column of Table 3.2 shows both cases.

Lemma 3.4 states that there is a MS decomposition  $\mathcal{M}(\mathcal{S}, \emptyset)$  of a discrete vector field  $(\mathcal{S}, \emptyset)$  which corresponds to the MS decomposition  $M(S, X)$  of  $(S, X)$ . Then the 4-saddle point  $p$  and  $q$  correspond to a face  $f$  and a vertex  $v$  of  $\mathcal{S}$ , respectively. Thus, the cancellation between  $p$  and  $q$  can be represented in  $\mathcal{S}$  as a matching  $\{v, d\}$  between the vertex  $v$  and the diagonal  $d$  of a face  $f$ , producing a discrete vector field  $(\mathcal{S}, \{v, d\})$ ; Table 3.2 shows this matching on its second column, considering two bipartitions of  $\mathcal{S}$ .

We provide another connection between discrete vector fields and Morse matchings related to duality. A discrete vector field  $(\mathcal{S}, \{v, d\})$  encodes both a singleton Morse matching  $\{v, d\}$  on the decomposition  $\mathcal{S}_1$  and a singleton Morse matching  $\{v^*, d^*\}$  in its dual decomposition  $\mathcal{S}_1^*$ , where  $\mathcal{S}_1$  and  $\mathcal{S}_1^*$  are provided by Theorem 2.2 applied to  $\mathcal{S}$ . Thus, the discrete vector field  $(\mathcal{S}, \{v, d\})$  encodes a Morse matching and its dual (defined in Appendix A) in the same structure. Table 3.2 shows both cases on its last column.

We now analyze the behavior of the discrete vector field  $(\mathcal{S}, \{v, d\})$

MS vector field	Discrete vector field	Morse matching

Table 3.2: First column: the possible cancellations of two critical points in a MS vector field. Second column: the possible matchings between a vertex and a face diagonal in a bipartite 4-decomposition. Last column: the possible Morse matchings on the two decompositions given by this bipartite 4-decomposition.

(Figure 3.7(a)) under the cancellation of the critical points  $p$  and  $q$  of  $(S, X)$ . Applying Theorem 3.3 to the points  $p$  and  $q$  of  $(S, X)$  (Figure 3.5(a)), we obtain a simple MS vector field (Figure 3.5(b)) which provides a MS decomposition. From Lemma 3.4, such a decomposition corresponds to a MS decomposition of a new discrete vector field (Figure 3.7(b)). The conclusion is that  $(\mathcal{S}, \{v, d\})$  is equivalent (this can be formalized somehow) to  $\mathcal{S}$  with a cancellation between the vertex  $v$  and the face  $f$  (Figure 3.7). This is exactly what Theorem A.1 would provide if applied to the Morse matching  $\{v, d\}$  on  $\mathcal{S}_1$ .

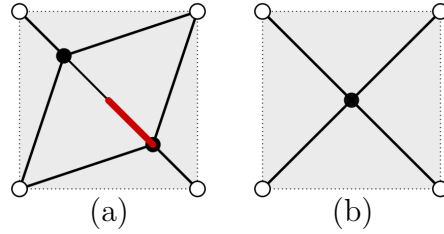


Figure 3.7: (a) a matching between a vertex and a face diagonal. (b) the resulting bipartite 4-decomposition after cancellation of the matched cells.

### The general matching

To introduce the general case of a discrete vector field, we apply induction on the previous construction for a singleton matching. Consider the set  $P = \{\{p_1, q_1\}, \{p_2, q_2\}, \dots, \{p_k, q_k\}\}$  of disjoint pairs of critical points in a MS vector field  $(S, X)$ , such that for each  $1 \leq i \leq k$ ,  $p_i$  and  $q_i$  are connected by a unique separatrix.

Applying Morse cancellation on the pair  $\{p_1, q_1\}$  of critical points of  $(S, X)$ , we obtain a MS vector field containing the set  $\{\{p_2, q_2\}, \dots, \{p_k, q_k\}\}$  of

disjoint pairs of critical points. To cancel  $\{p_2, q_2\}$  we must verify that this pair is connected by a unique separatrix, since  $\{p_1, q_1\}$  and  $\{p_2, q_2\}$  could configure the vertices of a cycle in the original MS decomposition. To avoid this test, we suppose that  $P$  is an acyclic matching. By induction, the pairs in  $P$  can be canceled; there is no ambiguity in choosing different orders of cancellation.

Using the construction in the previous section, the acyclic matching  $P$  can be, inductively, replaced by a matching  $\mathcal{X} = \{\{v_1, d_1\}, \{v_2, d_2\}, \dots, \{v_k, d_k\}\}$  between vertices  $v_i$ 's and face diagonals  $d_i$ 's of a bipartite 4-decomposition  $\mathcal{S}$  of the surface  $S$ . This motivates a discrete definition for vector fields. A *discrete (acyclic) vector field* on a compact surface  $S$  is a pair  $(\mathcal{S} = (V, E, F), \mathcal{X})$  satisfying the following properties.

- i)  $\mathcal{S}$  is a decomposition of  $S$  consisting of only 3- and 4-gons;
- ii)  $\mathcal{X}$  consists of an acyclic matching  $\{\{v_1, e_1\}, \{v_2, e_2\}, \dots, \{v_k, e_k\}\}$  between the vertices  $v_i$ 's and the edges  $e_i$ 's of  $\mathcal{S}$ ;
- iii) The embedding of  $(V, E - \{e_1, e_2, \dots, e_k\})$  in  $S$  produces a bipartite 4-decomposition of  $S$ .

The discrete vector field  $(\mathcal{S}, \mathcal{X})$  corresponds to a MS vector field  $(S, X)$  and to an acyclic matching  $P$  in  $M(S, X)$ , as described above. Then, applying Morse cancellation, inductively, to each pair of critical points of  $P$  in  $(S, X)$ , we obtain a new MS vector field  $(S, X')$ . This has a MS decomposition  $M(S, X')$  which Lemma 3.4 states to be equivalent to a MS decomposition  $\mathcal{M}(\overline{\mathcal{S}}, \emptyset)$  of a discrete vector field  $(\overline{\mathcal{S}}, \emptyset)$ . In other words,  $(\mathcal{S}, \mathcal{X})$  corresponds to  $(\overline{\mathcal{S}}, \emptyset)$  and the vertices and faces of  $\overline{\mathcal{S}}$  correspond to the critical points of  $(S, X)$ .

### 3.2.1

#### Critical elements and topological properties

A vertex  $v$  in a discrete vector field  $(\mathcal{S}, \mathcal{X})$  is *critical* if it is unmatched in  $\mathcal{X}$ . The index of a vertex  $v$  is 1 if it is critical and 0 otherwise. Let  $c(f)$  be the number of unmatched edges in the boundary walk of a face  $f$ . We say that  $f$  is *critical* if  $c(f) \neq 2$ . Its index is  $1 - \frac{c(f)}{2}$ .

Property iii of a discrete vector field  $(\mathcal{S}, \mathcal{X})$ , where  $\mathcal{S} = (V, E, F)$ , says that  $(V, E - \{e_1, e_2, \dots, e_k\})$  is bipartite, where  $\{e_1, e_2, \dots, e_k\}$  are the matched edges. Then,  $V$  can be partitioned into white and black vertices. We take the following convention. The critical white (black) vertices correspond to minima (maxima) of a smooth vector field (Table 3.3).

For a face  $f$ , note that Property i of  $(\mathcal{S}, \mathcal{X})$  ensures that  $f$  is either a 4-gon or a 3-gon. Then  $c(f) \leq 4$ . We investigate the possibilities.

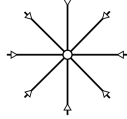
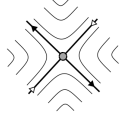
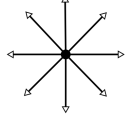
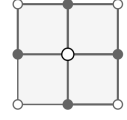
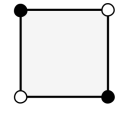
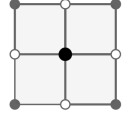
Index	1	-1	1
MS vector field	 Minimum	 4-saddle point	 Maximum
Discrete vector field	 White vertex	 4-gon	 Black vertex

Table 3.3: Correspondence presented in Table 3.1 increased by the indices of the critical elements.

- If  $c(f) = 4$ , then Properties **i** and **iii** imply that  $f$  is a 4-gon, since otherwise the embedding of the subgraph induced by the unmatched edges of  $(\mathcal{S}, \mathcal{X})$  would produce a face with more than 4 edges in the boundary walk. Hence  $f$  is a critical face with index  $-1$ ;
- If  $c(f) < 4$ , then Property **i** implies that  $f$  is a 3-gon. By Property **ii**  $c(f) \neq 3$  and by Property **iii**  $c(f) = 2$ ; analogous to previous item. Hence  $f$  is a regular face with index 0.

Thus the critical faces in  $(\mathcal{S}, \mathcal{X})$  are 4-gons with index  $-1$ : they correspond to 4-saddle points of a smooth vector field, as shown in the middle column of Table 3.3. We reinterpret Forman's version of the Euler-Poincaré formula [23].

**Theorem 3.5 (Forman [23])** *Let  $(\mathcal{S} = (V, E, F), \mathcal{X})$  be a discrete vector field on a compact surface  $S$ . Then*

$$\chi(S) = \sum_{v \in V} \text{index}(v) + \sum_{f \in F} \text{index}(f).$$

The proof of Theorem 3.5 will be a particular case of Theorem 4.7, which will be proven in Chapter 4. We also reinterpret Forman's discrete version (Theorem A.1) of the fundamental theorem of classical Morse theory [36].

**Theorem 3.6 (Forman [23])** *The decomposition  $\mathcal{S}$  of a discrete vector field  $(\mathcal{S}, \mathcal{X})$  is homotopy equivalent to a decomposition  $\overline{\mathcal{S}}$  of a discrete vector field  $(\overline{\mathcal{S}}, \emptyset)$  whose  $p$ -cells, for  $p = 0, 2$ , are the critical  $p$ -cells of  $(\mathcal{S}, \mathcal{X})$ , and their indices are preserved.*

The proof of Theorem 3.6 is a particular case of Theorem 4.8, which will be proven in Chapter 4. Next we study the structure of a discrete vector field  $(\mathcal{S}, \mathcal{X})$  on a compact surface. By Theorem 3.6, the critical cells of  $(\mathcal{S}, \mathcal{X})$

produce a simple decomposition  $\overline{\mathcal{S}}$  of  $S$ . We define the *MS decomposition* of  $(\mathcal{S}, \mathcal{X})$  as the bipartite 4-decomposition of  $\overline{\mathcal{S}}$ , and it is denoted by  $\mathcal{M}(\mathcal{S}, \mathcal{X})$ . Two discrete vector fields  $(\mathcal{S}_1, \mathcal{X}_1)$  and  $(\mathcal{S}_2, \mathcal{X}_2)$  are said to be equivalent if  $\mathcal{M}(\mathcal{S}_1, \mathcal{X}_1)$  and  $\mathcal{M}(\mathcal{S}_2, \mathcal{X}_2)$  are equivalent, and  $[(\mathcal{S}_1, \mathcal{X}_1)]$  denotes the equivalence class of  $(\mathcal{S}_1, \mathcal{X}_1)$ .

We provide an explicit construction for the MS decomposition  $\mathcal{M}(\mathcal{S}, \mathcal{X})$  of  $(\mathcal{S}, \mathcal{X})$  (Figure 3.8). The basic ingredient is a *path*, inspired on Forman's definition [23]. This is a sequence of vertices in  $\mathcal{S}$ ,  $v_1 v_2 v_3 \dots v_k$ , such that for each  $1 \leq i < k$ , there is an edge  $e = v_i v_{i+1}$  satisfying  $\{v_i, e\} \in \mathcal{X}$ ; the highlighted paths in Figure 3.8(b) are paths of  $(\mathcal{S}, \mathcal{X})$ . The paths are the discrete counterpart of the orbits in continuous vector fields.

As in smooth vector field (Section 3.1) we define a graph  $\mathcal{M}$ , where its vertices are the critical cells of  $(\mathcal{S}, \mathcal{X})$  (the red cells in Figure 3.8(a)). We create an edge between a critical face  $f$  and a critical vertex  $v$  for each path, with no edge in  $f$ , which connects  $v$  with a vertex in  $f$ 's boundary walk (the highlighted paths in Figure 3.8(b)). The orientability of the underlying surface  $S$  induces a rotational system  $\mathcal{R}$ . Thus the MS decomposition  $\mathcal{M}(\mathcal{S}, \mathcal{X})$  is given by Theorem 2.1 applied to  $\mathcal{M}$  and  $\mathcal{R}$ . Algorithm 1 provides an explicit construction for the faces of  $\mathcal{M}(\mathcal{S}, \mathcal{X})$ .

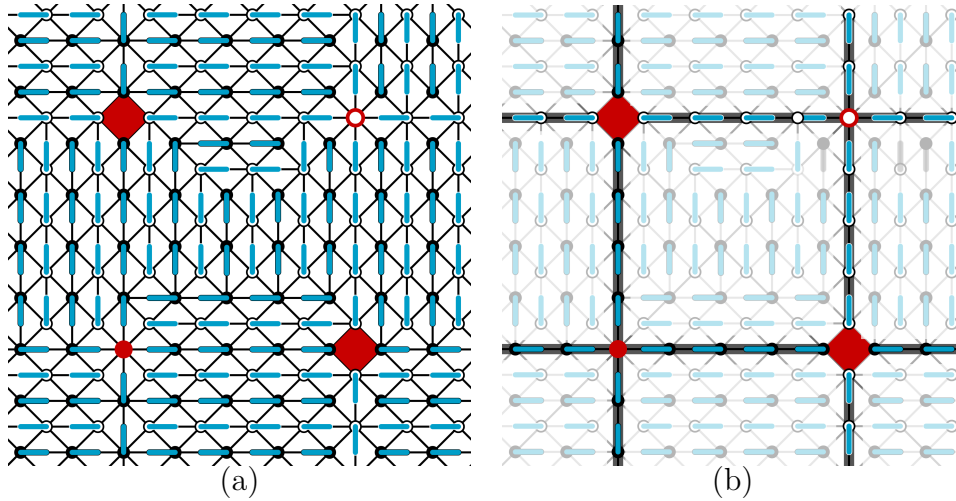


Figure 3.8: (a) a discrete vector field, the critical cells are in red. (b) the MS decomposition of (a).

### 3.2.2

#### Smooth vector fields and discrete vector fields

We now build a correspondence between the equivalence classes of discrete and smooth vector fields. From an equivalence class  $[(\mathcal{S}, \mathcal{X})]$  of a discrete vector field  $(\mathcal{S}, \mathcal{X})$ , we obtain a MS decomposition  $\mathcal{M}(\mathcal{S}, \mathcal{X})$  of

the underlying surface, essentially, by Theorem 3.6. On the other hand, by Theorem 3.2, the equivalence class under topological equivalence  $[(S, X)]$  of a vector field  $(S, X)$  corresponds to a MS decomposition  $M(S, X)$ . Finally, Lemma 3.4 gives the identification between  $M(S, X)$  and  $\mathcal{M}(\mathcal{S}, \mathcal{X})$ , since  $\mathcal{M}(\mathcal{S}, \mathcal{X})$  is by construction equivalent to  $\mathcal{M}(\overline{\mathcal{S}}, \emptyset)$ .

$$[(\mathcal{S}, \mathcal{X})] \xleftarrow{\text{Thm 3.6}} \mathcal{M}(\mathcal{S}, \mathcal{X}) \xleftarrow{\text{Lem 3.4}} M(S, X) \xleftarrow{\text{Thm 3.2}} [(S, X)] \quad (3.4)$$

The identification is Diagram 3.1. It implies that discrete vector fields are in correspondence with the topological aspects of MS vector fields.

**Corollary 3.7 (Forman [23])** *Every equivalence class of MS vector fields has a MS decomposition isomorphic to a bipartite 4-decomposition, which in turn corresponds to an equivalence class of discrete vector fields.*

Corollary 3.7 is not actually presented by Forman [23], but it is straightforward once we have Theorem 3.2 [17] and Theorem 3.6 [23]. Next we present a connection between Morse matchings and discrete vector fields.

### 3.2.3

#### Discrete vector fields and Morse matchings

We finish this chapter describing an algorithmic procedure to bridge Morse matchings (Appendix A) and discrete vector fields. This ensures that the definition of discrete vector fields is indeed codifying Morse matchings (through a different representation). Such algorithmic procedure may be used to build discrete vector fields by translating the Morse matching constructions in the literature [29, 37, 38, 39, 40, 41, 42, 43] to discrete vector fields.

Let  $\mathcal{S}$  be a decomposition of a compact surface  $S$ , and  $\mathcal{X}$  be a Morse matching on  $\mathcal{S}$  (as in Figure 3.9(a)). We construct a discrete vector field on the bipartite 4-decomposition  $\mathcal{M}(\mathcal{S})$  of  $\mathcal{S}$  based on  $\mathcal{X}$ . Let  $W \sqcup B$  be a bipartition of  $\mathcal{M}(\mathcal{S})$  vertices's, where  $W$  are the white vertices and  $B$  are the black vertices. The construction of  $\mathcal{M}(\mathcal{S})$  (presented in Section 2.1) provides a bijection between the faces, vertices, and edges of  $\mathcal{S}$  and the white vertices, black vertices, and faces of  $\mathcal{M}(\mathcal{S})$ , respectively (Figure 3.9(b)).

Let  $\{\sigma, \tau\} \in \mathcal{X}$  be a matching between an edge  $\sigma$  and a face (vertex)  $\tau$  (Figure 3.9(a)). In  $\mathcal{M}(\mathcal{S})$ ,  $\sigma$  and  $\tau$  correspond to a face  $f$  and a white (black) vertex  $w$ , respectively (Figure 3.9(b)). Match  $w$  and its adjacent diagonal  $e$  of  $f$  (Figure 3.9(c)) creating  $\{w, e\}$ . Repeating this construction for each matching in  $\mathcal{X}$  we build a Morse matching  $\mathcal{X}'$  between vertices and face diagonals in  $\mathcal{M}(\mathcal{S})$ . Then adding these face diagonals to the decomposition  $\mathcal{M}(\mathcal{S})$  we



obtain a decomposition  $\mathcal{M}(\mathcal{S})'$  which together with  $\mathcal{X}'$  provide the desired discrete vector field  $(\mathcal{M}(\mathcal{S})', \mathcal{X}')$  (Figure 3.9(c)).

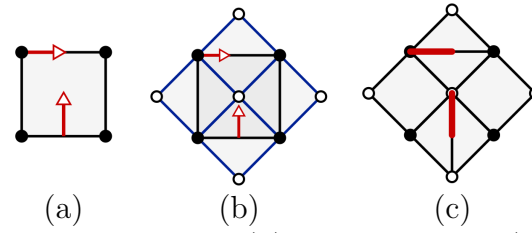
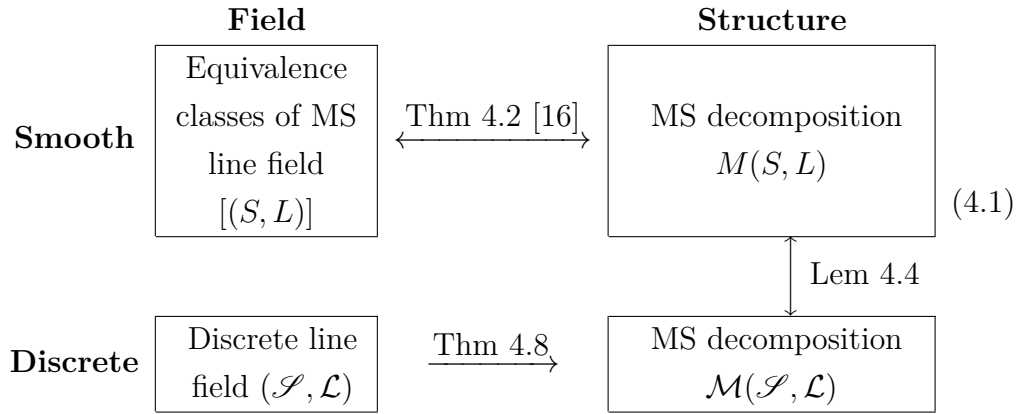


Figure 3.9: (a) a Morse matching. (b) the overlap of (a) by its bipartite 4-decomposition. (c) the corresponding discrete vector field.

## 4

### Line fields

In this chapter we generalize the definitions and results of the previous chapter to line fields. In particular, we define discrete line fields in a way that entails the discrete vector field structure presented in Section 3.2. We follow Diagram 4.1, informally presented in Chapter 1.



The chapter has two sections. In the first, we start by defining the concepts of a MS line field  $(S, L)$  (upper left box of Diagram 4.1) on a compact surface  $S$ , and the MS decomposition  $M(S, L)$  (upper right box of Diagram 4.1) of the field  $(S, L)$ . We conclude the section by presenting Theorem 4.2 [16] which states a correspondence between  $(S, L)$  and  $M(S, L)$ . The second section introduces the analogous discrete concepts of a MS line field and Theorem 4.8. We also present an identification between the MS decompositions of smooth and discrete line fields (Lemma 4.4).

The main goal of this chapter is Corollary 4.9, yielding the correspondence between MS line fields and discrete line fields [23].

#### 4.1

##### Smooth line fields

In this section, we summarize the theory of MS line fields [16, 20, 24, 25, 44]. Let  $S$  be a compact and orientable surface, and  $TS$  its tangent bundle. Define an equivalence relation in  $TS$ , where two elements  $(p_1, v_1)$  and  $(p_2, v_2)$  are equivalent if  $\pi(p_1, v_1) = \pi(p_2, v_2)$  and  $v_1 = \pm v_2$ . In this case, we denote

$(p_1, v_1) \sim (p_2, v_2)$ . This equivalence provides a fiber bundle  $LS = TS / \sim$  with a natural projection  $\lambda := \pi / \sim$  over  $S$ . A *line field* is a pair  $(S, L)$ , where  $L : S \rightarrow LS$  is a smooth map satisfying  $\lambda \circ L = Id$ .

As in vector fields, a point  $p$  in a line field  $(S, L)$  is said to be *critical* if  $L(p) = (p, 0)$ . A curve  $\gamma : (a, b) \rightarrow S$ , with  $a < b$ , is an *integral line* of  $(S, L)$  if  $\gamma'(t) \in L(\gamma(t))$  for  $t \in (a, b)$ . The integral line  $\gamma$  is an *orbit* of  $(S, X)$  if it is a maximal integral line. The field  $(S, L)$  is called *acyclic* when it does not admit an orbit  $\gamma$  which is a closed curve.

As for vector fields, two fields  $(S, L_1)$  and  $(S, L_2)$  are *topologically equivalent* if there is a homeomorphism  $h : S \rightarrow S$  mapping orbits from  $(S, L_1)$  to orbits of  $(S, L_2)$ . The equivalence class of  $(S, L_1)$  is denoted by  $[(S, L_1)]$ .

A line field  $(S, L)$  is *structurally stable* if it admits an open neighborhood in the space of line fields consisting of topologically equivalent line fields. Bronshteyn and Nikolaev [24] proved that the critical points in a structurally stable line field are necessarily of the form of those listed in Figure 4.1.

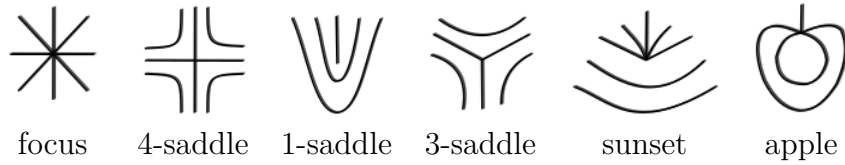


Figure 4.1: The list of all structurally stable critical points allowed in a smooth line field. The last four types of critical points are not present in line fields.

To extend Properties **i** - **iii** of a MS vector field (Section 3.1) to an (acyclic) line field  $(S, L)$  Bronshteyn and Nikolaev [24] replace the sunset points (the fifth type listed in Figure 4.1) by pairs consisting of focus and 3-saddle points. The apple points (the last type listed in Figure 4.1) are also replaced by focus and 1-saddle points. Finally, they define a MS line field as an line field  $(S, L)$  satisfying:

- i)** There are finitely many critical points, being necessarily focus, 4-saddle, 1-saddle, and 3-saddle points (first four types listed in Figure 4.1);
- ii)** There is no orbits between two critical points;
- iii)** The limit sets of each orbit are critical points (there are no closed orbits).

Fields satisfying these properties are called *MS* (Figure 4.2(a)). Bronshteyn and Nikolaev [24] extended Theorem 3.1 to line fields.

**Theorem 4.1 (Bronshteyn–Nikolaev [24])** *Structurally stable line fields are in bijection with MS line fields. Further, they form an open and dense subset of the space of smooth line fields.*

The second part of Theorem 4.1, informally, states that every line field is a small perturbation of a MS line field. This result is not used in the constructions in this work, but it provides robustness to the definition of MS line fields.

### MS decomposition

Theorem 4.1 invites for a combinatorial description of structurally stable line fields, since it produces a correspondence between such fields and MS line fields, which in turn satisfy the combinatorial Properties **i** - **iii**. They state that a MS line field has finitely many critical points and they are all connected by *separatrices*: the orbits which have a saddle point as limit set (Properties **ii** and **iii**). As we observed for vector fields in Chapter 3, this suggests a representation of a MS vector field  $(S, X)$  by a decomposition of the underlying surface. However, as mentioned by Bronshteyn and Nikolaev [24], additional constructions are necessary.

We say that a line field  $(S, L)$  is *orientable* if it is possible to construct a vector field  $(S, X)$  such that  $X(p) \in L(p) = \{(p, v), (p, -v)\}$  for each  $p \in S$ , and *non-orientable* otherwise [18]. Clearly, the orientable MS line fields are MS vector fields, so we only need to treat the non-orientable MS line fields.

In a tradition dating back to the construction of Riemann surfaces, Bronshteyn and Nikolaev [16] studied a non-orientable MS line field  $(S, L)$  by considering a triple  $(\tilde{S}, X, \theta)$  (Figure 4.2) defined over a double branched covering  $\tilde{S}$  of  $S$ . The branch points coincide with the non-orientable critical points. Such triple must satisfy the following properties.

- i)  $\theta$  is an involution in  $\tilde{S}$  preserving orbits of the vector field  $(\tilde{S}, X)$ , and the quotient  $(\tilde{S}/\theta, X/\theta)$  is topologically equivalent to  $(S, L)$ ;
- ii)  $\theta$  fixes only a finite number of critical points that when projected to  $\tilde{S}/\theta$  corresponds to 1-saddle and 3-saddle points;
- iii) There is no orbits between saddle points.

The triple  $(\tilde{S}, X, \theta)$  provides an *orgraph*  $\tilde{M} = (\tilde{V}, \tilde{E})$ , as it did in Section 3.1 for MS vector fields. The vertices  $\tilde{V}$  are the critical points of  $(\tilde{S}, X)$ . The separatrices between the critical points make up the set of edges  $\tilde{E}$ . The orgraph  $\tilde{M}$  is a tripartite graph, consisting of an upper level of maxima, a lower level of minima, and a middle level containing the 2-, 4-, and 6-saddles of  $(\tilde{S}, X)$ . The orientation of  $\tilde{S}$  provides a rotational system on  $\tilde{M}$  and then Theorem 2.1 induces a decomposition of  $\tilde{S}$ , named *MS decomposition* of  $(\tilde{S}, X, \theta)$  and denoted by  $\tilde{M}(\tilde{S}, V, \theta)$ . Figure 4.3(a) illustrates the MS decomposition of the triple presented in Figure 4.2(b). A decomposition

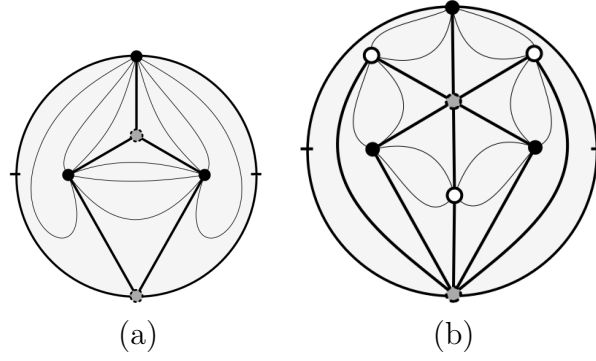


Figure 4.2: (a) a MS line field with two 3-saddle and three focus points on the sphere. (b) the suspension of the MS line field; white (black) dots represent the minima (maxima).

enjoying the properties of a MS decomposition of a line field is called an *abstract MS decomposition*. The following result is a line field analogous to Theorem 3.2.

**Theorem 4.2 (Bronshteyn–Nikolaev [16])** *Two MS line fields are topologically equivalent if and only if they admit equivalent MS decompositions. Moreover, every abstract MS decomposition is equivalent to a MS decomposition of a MS line field.*

$$\begin{array}{ccc} \text{MS line field} & \xleftrightarrow{\text{Theorem 4.2 [16]}} & \text{MS decomposition} \\ [(\tilde{S}, X, \theta)] & & M(\tilde{S}, X, \theta) \end{array} \quad (4.2)$$

The branched covering double the cells of the MS decomposition  $M(\tilde{S}, X, \theta)$  of  $(\tilde{S}, X, \theta)$ , except at branched points. We can reduce the complexity of computing  $M(\tilde{S}, X, \theta)$  by avoiding this doubling of cells. To this end, we define the *MS decomposition*  $M(S, L)$  of the field  $(S, L)$  as the projection of  $M(\tilde{S}, X, \theta)$  on  $S$  by the 2-branched covering  $p : \tilde{S} \rightarrow S$  (Figure 4.3).

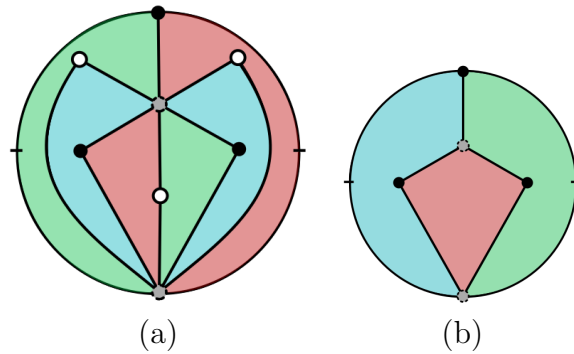


Figure 4.3: (a) the MS decomposition of the triple presented in Figure 4.2(b). (b) the MS decomposition of the line field given in Figure 4.2(a).

The MS decomposition  $M(S, L)$  of a MS line field  $(S, L)$  enjoys the following properties [16].

- a) The orgraph  $M$  is bipartite by two different sets, the focus, and the saddles of  $(S, L)$ ;
- b) Its faces are 4-gons;
- c) The  $n$ -saddle vertices have  $n$  connections with the focus vertices;
- d) If there is no saddle vertex, then  $M(S, L)$  is a decomposition of the sphere consisting of a unique 2-gon (special case).

Item **a** follows from Property **i** of MS line fields. Property **b** is Lemma 4.4, which we prove in the next section. Item **c** follows from Properties **i** - **ii** of MS line fields. Figure 1.1 presented in the introduction of this thesis is an expressive example of a MS decomposition. As the triple  $(\tilde{S}, X, \theta)$  corresponds to  $(S, L)$ , Diagram (4.2) can be presented as follows.

$$\begin{array}{ccc} \text{MS line field} & \xleftrightarrow{\text{Theorem 4.2 [16]}} & \text{MS decomposition} \\ [(S, L)] & & M(S, L) \end{array} \quad (4.3)$$

The proof [16] that every abstractly given MS decomposition corresponds to a MS line field (second part of Theorem 4.2 ) does not depend on the number of separatrices having  $n$ -saddle as limit set. To allow the employment of  $n$ -saddle points,  $n \geq 5$ , for modeling purposes, we extend the definition of line fields.

A (*generalized*) MS line field  $(S, L)$  on an orientable compact surface  $S$  is a line field satisfying the MS properties **i** - **iii** (described above Theorem 4.1) with the set of critical points, described by Figure 4.1, increased by  $n$ -saddle points, with  $n > 4$  (Figure 4.4). Its MS decomposition  $M(S, L)$  is built as in the previous case.

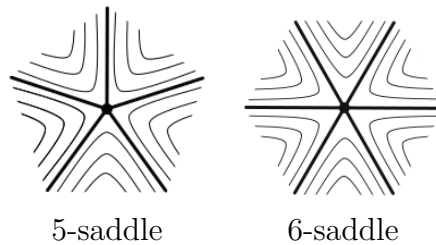


Figure 4.4: The saddles allowed in generalized MS line fields.

From now on the MS line fields will be treated as generalized MS line field. The next result is an extension of the second part of Theorem 4.2.

**Corollary 4.3** *Every abstract MS decomposition of a surface is equivalent to a MS decomposition of a MS line field.*

## 4.2

### Discrete line fields

The results presented in this section can also be found in [45], and they describe the main object of this work — the discrete line field — which is a generalization of the discrete vector field given in Section 3.2.

The key idea, again, is to replace a smooth (acyclic) line field  $(S, L)$  on the compact (possible orientable) surface  $S$  by a pair  $(\mathcal{S}, \mathcal{L})$ , called *discrete (acyclic) line field*, which consists of a decomposition  $\mathcal{S}$  of  $S$ , and a Morse matching  $\mathcal{L}$  between vertices and edges of  $\mathcal{S}$ . Observe that no restriction is imposed in  $\mathcal{S}$ . Meanwhile, the underlying decomposition of a discrete vector field is a bipartite 4-decomposition. To analyze a discrete line field  $(\mathcal{S}, \mathcal{L})$ , we start with an empty matching ( $|\mathcal{L}| = 0$ ), then we consider a singleton matching ( $|\mathcal{L}| = 1$ ), and to conclude we analyze a general matching.

### Empty matching

To analyze a discrete line field  $(\mathcal{S}, \emptyset)$ , we consider  $\mathcal{M}(\mathcal{S}, \emptyset)$  be its bipartite 4-decomposition of  $\mathcal{S}$ , as stated in Theorem 2.2 (Figures 4.5(a)-(d)). This decomposition, naturally, satisfies the following properties.

- a) The vertices and the faces of  $\mathcal{S}$  induce a bipartition of the vertices in  $\mathcal{M}(\mathcal{S}, \emptyset)$ ;
- b) The faces of  $\mathcal{M}(\mathcal{S}, \emptyset)$  are 4-gons;
- c) The vertices of  $\mathcal{M}(\mathcal{S}, \emptyset)$  which represents the  $n$ -gons of  $\mathcal{S}$  have  $n$  adjacencies with the vertices of  $\mathcal{M}(\mathcal{S}, \emptyset)$ ;
- d) If  $\mathcal{M}(\mathcal{S}, \emptyset)$  admits only two vertices, then it is a decomposition of the sphere consisting of two vertices connected by an edge (special case).

The decomposition  $\mathcal{M}(\mathcal{S}, \emptyset)$  is called *MS decomposition* of  $(\mathcal{S}, \emptyset)$ . Properties **a** - **d** are identical to Properties **a** - **d** of the MS decomposition of a MS line field. For instance, compare Figures 4.3(b) and 4.5(d). The following lemma states this correspondence.

**Lemma 4.4** *The MS decomposition  $\mathcal{M}(\mathcal{S}, \emptyset)$  of a discrete line field  $(\mathcal{S}, \emptyset)$  is equivalent to the MS decomposition  $M(S, L)$  of a MS line field  $(S, L)$ .*

**Proof.** As said above, this proof follows directly from the fact that Properties **a** - **d** of  $\mathcal{M}(\mathcal{S}, \emptyset)$  are identical to Properties **a** - **d** of  $M(S, L)$ . However, the proof of Property **b** of  $M(S, L)$  is still missing. This property states that all the faces of  $M(S, L)$  are 4-gons. To verify this, let  $\Sigma$  be a face of  $M(S, L)$ . Then by Property **a** of  $M(S, L)$  the number of edges in the boundary walk of  $\Sigma$  is even. Now attach two copies of  $\Sigma$  along their boundary walk, which becomes an equator of a sphere  $\mathbb{S}^2$ . The line field map  $L$  restricted to the copies of  $\Sigma$  produces a line field  $(\mathbb{S}^2, L)$  with copies of the field in  $\Sigma$  on each hemisphere. In the sphere, the vertices of  $\Sigma$  which represent  $n$ -saddle points of  $L$  have index zero (they are removed by small perturbations) and the focus points are maintained. Since the Euler characteristic of  $(\mathbb{S}^2, L)$  is 2, the total number of focus points must be 2. In other words the face  $\Sigma$  is a 4-gon. ■

$$\begin{array}{ccc} \text{MS decomposition} & \xleftrightarrow{\text{Lemma 4.4}} & \text{MS decomposition} \\ \mathcal{M}(\mathcal{S}, \emptyset) & & M(S, L) \end{array} \quad (4.4)$$

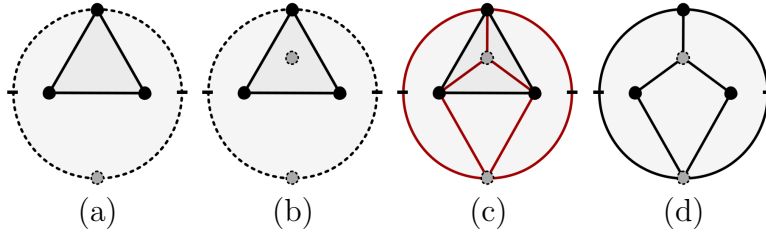


Figure 4.5: (a) a decomposition of the sphere into two triangles. (b) each triangle receives a grey point. (c) and (d) the bipartite 4-decomposition.

Corollary 4.3 and Lemma 4.4 provide a correspondence between the focus and the  $n$ -saddle points of a MS line field and the vertices and the  $n$ -gons of a decomposition, respectively; see Table 3.1 and Figure 4.6 for examples.

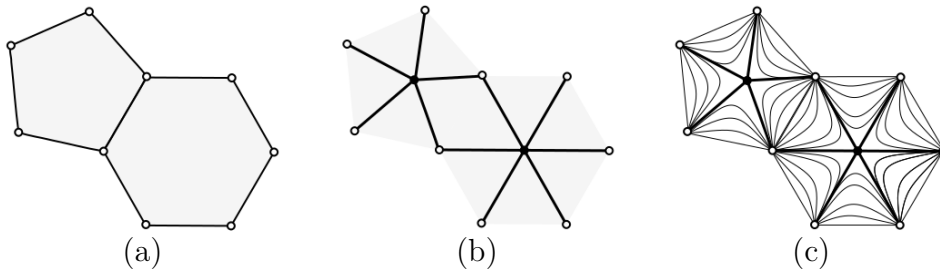


Figure 4.6: (a) a piece of a decomposition. (b) the associated bipartite quadrilateral embedding. (c) the corresponding line field.

### Singleton matching

To introduce a discrete line field  $(\mathcal{S}, \mathcal{L})$  with a singleton matching in  $\mathcal{L}$  we inspire in the definition of discrete vector fields. We set  $\mathcal{L}$  as a matching  $\{v, e\}$



between a vertex  $v$  and an adjacent regular edge  $e$  (Figure 4.7(a)). However, we can not follow the ideas of Section 3.2, which uses the Morse cancellation theorem, since it only allows cancellation of critical points in vector fields [21]. To overcome this difficulty, we take an approach based on “collapses”.

**Lemma 4.5** *The decomposition  $\mathcal{S} = (V, E, F)$  of a discrete line field  $(\mathcal{S}, \{v, e\})$  is homotopy equivalent to a decomposition  $\overline{\mathcal{S}} = (V - v, E - e, F)$  where the faces adjacent to  $e$  have the pair  $\{v, e\}$  removed from their boundary walk.*

**Proof.** Let  $u$  be the endpoint of a regular edge  $e$  such that  $u \neq v$ . The pair  $\{v, e\}$  defines a Morse matching, since  $u$  is unmatched, and thus there is no alternated cycle containing  $\{v, e\}$ . Theorem A.1 applied to  $\mathcal{S}$  and  $\{v, e\}$  provides the desired decomposition. ■

Figures 4.7(a) and (b) give an example of the proof of Lemma 4.5.

The next step is to collapse the 2-gons of the decomposition. Indeed, from Lemma 4.4, they represent critical points in a MS line field with exactly 2 separatrices, and are thus collapsible.

**Lemma 4.6** *Let  $\mathcal{S} = (V, E, F)$  be a decomposition of a surface  $S$  and  $f$  be a face with boundary walk consisting of two distinct edges,  $e_1$  and  $e_2$ . Then  $\mathcal{S}$  is homotopy equivalent to a decomposition  $\overline{\mathcal{S}} = (V, E - e_1, F - f)$  of  $S$ .*

**Proof.** The pair  $\{e_1, f\}$  defines a Morse matching, since  $e_2$  is unmatched making it impossible the existence of an alternated cycle containing  $\{e_1, f\}$ . Theorem A.1 applied to  $\mathcal{S}$  and  $\{e_1, f\}$  provides the desired decomposition. ■

Figures 4.7(c) and (d) provide an illustration of the proof of Lemma 4.6.

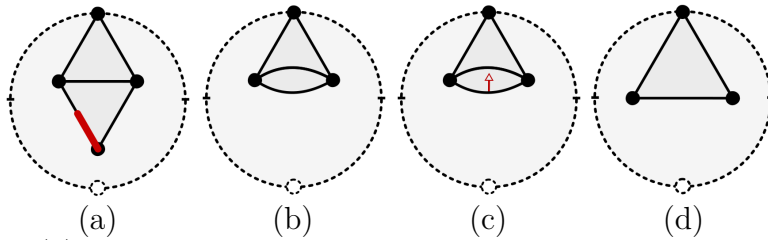


Figure 4.7: (a) presents a discrete line field with a singleton matching; (b) is the result of applying Lemma 4.5 to (a). Finally, Lemma 4.6 applied to (b) is expressed in (c) and (d).

### General matching

Lemmas 4.5 and 4.6 motivate a *discrete (acyclic) line field* on a compact surface  $S$  as a pair  $(\mathcal{S}, \mathcal{L})$  satisfying the following properties.

- i)  $\mathcal{S}$  is a decomposition of  $S$ ;
- ii)  $\mathcal{L}$  consists of an acyclic matching between vertices and edges of  $\mathcal{S}$ .

Items **i** - **ii** of a discrete line field are more general than Properties **i** - **iii** of a discrete vector field since no restriction on the underlying decomposition was imposed (Figure 4.8).

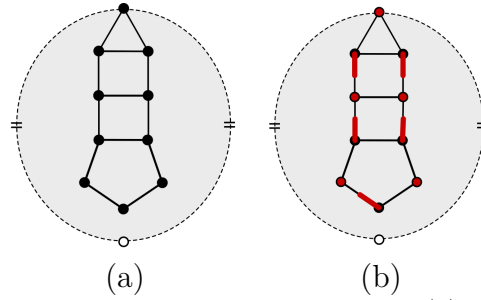


Figure 4.8: (a) a decomposition of the sphere. (b) a discrete line field. (c) a discrete line field.

We now present the definitions of critical elements and their indices for discrete line fields. The expected results still hold: a Euler–Poincaré formula and a homotopic characterization of the underlying decomposition, that is, the line field version of Theorems 3.5 and 3.6 as a reinterpretation of Forman’s Morse matching results [23].

#### 4.2.1

##### Critical elements and topological properties

A vertex  $v$  in a discrete line field  $(\mathcal{S}, \mathcal{L})$  is *critical* if it is unmatched in  $\mathcal{L}$ . The *index* of vertex  $v$  is 1 if it is critical and 0 otherwise. Let  $c(f)$  be the number of unmatched edges in the boundary walk of a face  $f$ . We say that  $f$  is *critical* if  $c(f) \neq 2$ . Its index is  $1 - \frac{c(f)}{2}$ . We denote the face  $f$  by  $c(f)$ -gon. In Figure 4.8(b), the pentagon is a 4-gon with index  $-1$ .

Next we present the first topological property for discrete line fields, the Euler–Poincaré formula.

**Theorem 4.7** *Let  $\mathcal{S} = (V, E, F)$  be a decomposition of the compact surface  $S$  and  $(\mathcal{S}, \mathcal{L})$  be a discrete line field. Then*

$$\chi(S) = \sum_{v \in V} \text{index}(v) + \sum_{f \in F} \text{index}(f).$$

For convenience, the proof will be provided after Theorem 4.8, the discrete line field version of Theorem 3.6. This result is based on Lemmas 4.5 and 4.6 and it states that the critical elements of a discrete line field contain the necessary information to characterize the homotopy type of its underlying decomposition (Figure 4.9 provides an illustration).

**Theorem 4.8** *The decomposition  $\mathcal{S}$  of a discrete line field  $(\mathcal{S}, \mathcal{L})$  is homotopy equivalent to a decomposition  $\overline{\mathcal{S}}$  of a line field  $(\overline{\mathcal{S}}, \emptyset)$  whose  $p$ -cells, for  $p = 0, 2$ , are the critical  $p$ -cells of  $(\mathcal{S}, \mathcal{L})$ , and their indices are preserved.*

**Proof.** By the definition of  $(\mathcal{S}, \mathcal{L})$ ,  $\mathcal{L}$  is a Morse matching between vertices and edges of  $\mathcal{S}$  (Figure 4.9(a)). Then, Theorem A.1 applied to  $\mathcal{L}$  produces a decomposition  $\mathcal{S}'$  (Figure 4.9(b)) homotopy equivalent to  $\mathcal{S}$ , whose vertices are the critical vertices of  $(\mathcal{S}, \mathcal{L})$ . We now observe that the non-critical faces have only two different edges on their boundary walk. Applying Lemma 4.6 to each of these possible non-critical faces of  $(\mathcal{S}', \emptyset)$  (Figure 4.9(c)), we obtain a decomposition  $\overline{\mathcal{S}}$  (Figure 4.9(d)) homotopy equivalent to  $\mathcal{S}'$  containing only the critical faces  $(\mathcal{S}, \mathcal{L})$ . ■

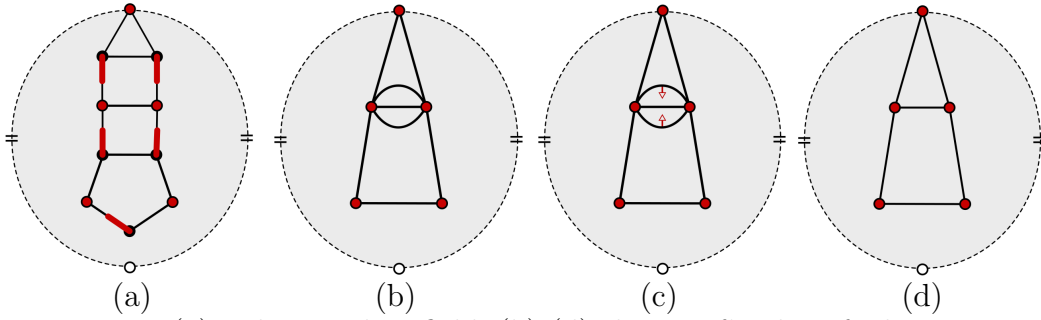


Figure 4.9: (a) a discrete line field. (b)-(d) the proof's idea of Theorem 4.8.

We now prove the Euler–Poincaré formula for a discrete line field.

**Proof of Theorem 4.7.** From Theorem 4.8, it is enough to prove the case  $\mathcal{L} = \emptyset$ . By Euler's formula of the decomposition  $\mathcal{S} = (V, E, F)$ ,

$$\chi(\mathcal{S}) = |V| - |E| + |F|.$$

Since all vertices are critical,  $|V| = \sum_{v \in V} \text{index}(v)$ . In the sum

$$\sum_{f \in F} \text{index}(f) = |F| - \sum_{f \in F} \frac{c(f)}{2},$$

each edge  $e \in E$  is counted twice in the boundary walk of the  $\mathcal{S}$  face's, since  $\mathcal{S}$  is a decomposition of a compact surface. Then  $\sum_{f \in F} \frac{c(f)}{2} = |E|$ . ■

Next we study the global structure of a discrete line field  $(\mathcal{S}, \mathcal{L})$ . By Theorem 4.8, the critical cells of  $(\mathcal{S}, \mathcal{L})$  produce a simple decomposition  $\overline{\mathcal{S}}$  of  $S$ . As we did for vector fields, we now define the *MS decomposition* of  $(\mathcal{S}, \mathcal{L})$  as the bipartite 4-decomposition of  $\overline{\mathcal{S}}$ , and it is denoted by  $\mathcal{M}(\mathcal{S}, \mathcal{L})$ . Two discrete line fields  $(\mathcal{S}_1, \mathcal{L}_1)$  and  $(\mathcal{S}_2, \mathcal{L}_2)$  are said to be equivalent if  $\mathcal{M}(\mathcal{S}_1, \mathcal{L}_1)$  and  $\mathcal{M}(\mathcal{S}_2, \mathcal{L}_2)$  are equivalent.  $[(\mathcal{S}_1, \mathcal{L}_1)]$  denotes the equivalence class of  $(\mathcal{S}_1, \mathcal{L}_1)$ . The next diagram is a discrete version of (4.3).

$$\begin{array}{ccc} \text{Discrete line} & \xleftrightarrow{\text{Theorem 4.8}} & \text{MS decomposition} \\ \text{field } [(\mathcal{S}, \mathcal{L})] & & \mathcal{M}(\mathcal{S}, \mathcal{L}) \end{array} \quad (4.5)$$

We now develop an explicit construction for the MS decomposition  $\mathcal{M}(\mathcal{S}, \mathcal{L})$  of  $(\mathcal{S}, \mathcal{L})$ . We follow the illustrations in Figures 4.10(a) and (b). A basic ingredient in this construction is based on *paths*, as in the case of discrete vector fields. Remarking, this is a sequence of vertices in  $\mathcal{S}$ ,  $v_1 v_2 v_3 \dots v_k$ , such that for each  $0 \leq i < k$  there is a edge  $e$ , which contains  $v_i$  and  $v_{i+1}$  satisfying  $\{v_i, e\} \in \mathcal{L}$ . The highlighted paths in Figure 4.10(b) are examples of paths.

We define a graph  $\mathcal{M}$ , whose vertices are the critical cells of  $(\mathcal{S}, \mathcal{L})$ . We create an edge between a critical face  $f$  and a critical vertex  $v$  for each path which connects  $v$  to a vertex in the boundary walk of  $f$  (Figure 4.10(b)). The orientability of the underlying surface  $S$  induces a rotational system  $\mathcal{R}$ . Thus the MS decomposition  $\mathcal{M}(\mathcal{S}, \mathcal{L})$  is given by Theorem 2.1 applied to  $\mathcal{M}$  and  $\mathcal{R}$ . Algorithm 1 provides an explicit construction for the faces of  $\mathcal{M}(\mathcal{S}, \mathcal{L})$ .

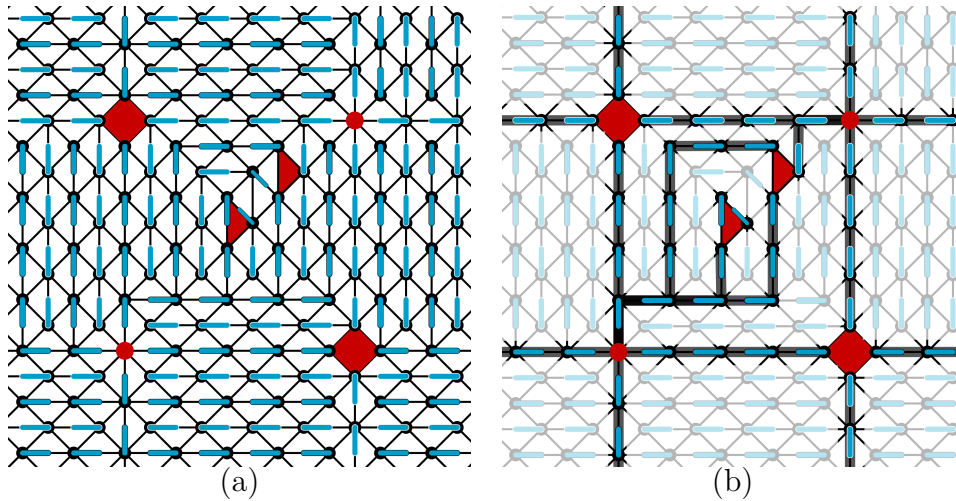


Figure 4.10: (a) a discrete line field, the critical cells are in red. (b) the MS decomposition of (a).

### 4.2.2

#### Smooth line fields and discrete line fields

We now build a correspondence between equivalence classes of discrete and continuous line fields. From an equivalence class  $[(\mathcal{S}, \mathcal{L})]$  of a discrete line field  $(\mathcal{S}, \mathcal{L})$ , we obtain a MS decomposition  $\mathcal{M}(\mathcal{S}, \mathcal{L})$  of the underlying surface by Theorem 4.8. On the other hand, by Theorem 4.2, the equivalence class under topological equivalence  $[(S, L)]$  of a line field  $(S, L)$  corresponds to a MS decomposition  $M(S, L)$ . Finally, Lemma 4.4 gives the identification between  $M(S, L)$  and  $\mathcal{M}(\mathcal{S}, \mathcal{L})$ , since it is by definition equivalent to  $\mathcal{M}(\overline{\mathcal{S}}, \emptyset)$ . These correspondences are related in (4.6)

$$[(\mathcal{S}, \mathcal{L})] \xleftarrow{\text{Thm 4.8}} \mathcal{M}(\mathcal{S}, \mathcal{L}) \xleftarrow{\text{Lem 4.4}} M(S, L) \xleftarrow{\text{Thm 4.2[16]}} [(S, L)] \quad (4.6)$$

The identification provided in Diagram 4.6 is Diagram 4.1 and it produces the following result, which guarantees that discrete line fields are in correspondence with the topological aspects of MS line fields.

**Corollary 4.9** *Every equivalence class of MS line field admits a MS decomposition equivalent to a bipartite 4-decomposition, which in turn corresponds to an equivalence class of discrete vector fields.*

See Figure 4.10 for an example of the correspondence stated in Corollary 4.9.

### 4.2.3

#### Discrete line fields and Morse matchings

In Subsection 3.2.3 we provided a correspondence between Morse matchings and discrete vector fields. Here, we use the less restrictive structure of discrete line fields to propose a more general definition of Morse matchings.

Let  $\mathcal{S}$  be a decomposition of a compact surface  $S$ , and  $\mathcal{X}$  be a Morse matching on  $\mathcal{S}$  (Figure 4.11(a)). In Subsection 3.2.3, we constructed a discrete vector field  $(\mathcal{M}(\mathcal{S})', \mathcal{X}')$ , based in the bipartite 4-decomposition  $\mathcal{M}(\mathcal{S})$  of  $\mathcal{S}$  and in  $\mathcal{X}$  (Figures 4.11(a)-(c)). The unmatched edges in  $\mathcal{M}(\mathcal{S})'$  correspond to the edges of  $\mathcal{M}(\mathcal{S})$ , which represent the adjacencies between the vertices and faces of  $\mathcal{S}$ . The matched edges correspond to the matching  $\mathcal{X}$ .

Let  $W$  and  $B$  be a bipartition of  $V$  of  $\mathcal{M}(\mathcal{S})$  in white and black vertices. A path  $\gamma$  in the discrete vector field  $(\mathcal{M}(\mathcal{S})', \mathcal{X}')$  connects either white vertices or black vertices, since the matched edges of  $\mathcal{M}(\mathcal{S})'$  are diagonals of a bipartite 4-decomposition (Figure 4.11(c)). As the unmatched edges are the edges of  $\mathcal{M}(\mathcal{S})$ , they have an endpoint in  $W$  and other in  $B$ . Then, adding a possible pair  $\{v, e\}$  of unmatched vertex and edge to discrete vector field

$(\mathcal{M}(\mathcal{S})', \mathcal{M}')$ , we obtain a discrete line field  $(\mathcal{M}(\mathcal{S})', \mathcal{L})$ , where  $\mathcal{L} = \{v, e\} \cup \mathcal{X}'$  (Figure 4.11(c) and (d)). A path containing  $\{v, e\}$  has both white vertices and black vertices (Figure 4.11(d)).

The black (white) vertices of  $\mathcal{M}(\mathcal{S})$  match with the vertices (faces) of  $\mathcal{S}$ , as observed in Subsection 3.2.3. Then, considering  $v$  as a black (white) vertex, the pair  $\{v, e\}$  corresponds to a matching, in  $\mathcal{S}$ , between a vertex  $v$  (face  $f$ ) and an adjacency between  $v$  ( $f$ ) and a face (vertex) (Figure 4.11(e)). This observation allows us to generalize Morse matchings by adding possible pairs of vertices (faces) and their adjacencies with faces (vertices).

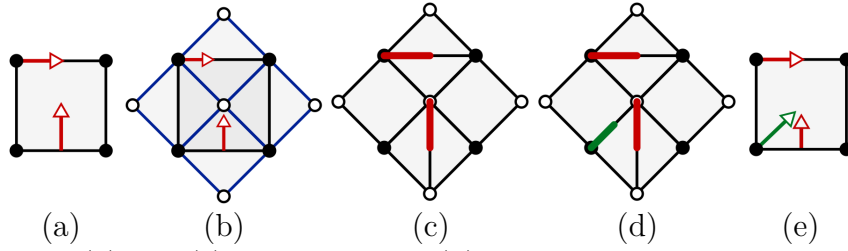


Figure 4.11: (a) and (c) are Figure 3.9. (d) adding a matching between a vertex and edge; (e) the matching on the original decomposition.

### 4.3

#### Cancellation in discrete line fields

We also propose a consistent (Morse-like) cancellation of critical elements in a discrete line field yielding a substantial simplification of the field without altering the topological type of the underlying surface. The proposal consists of two approaches: a merge between two critical faces connected by a unique strip of regular faces, and a cancellation between a critical face and a critical vertex connected by a unique path.

**Proposition 4.10** *Let  $f$  and  $g$  be critical faces of a discrete line field  $(\mathcal{S}, \mathcal{L})$ , which belong to a unique face  $\Lambda$  of  $\mathcal{M}(\mathcal{S}, \mathcal{L})$ . Then such faces can be merged into a unique critical face.*

**Proof.** Basically, it consists of the removal of the unmatched edges inside  $\Lambda$  (Figures 4.12(a) and (b)). More precisely, observe that the faces  $f$  and  $g$  share a unique edge  $a$  in  $\overline{\mathcal{S}}$ , since they are opposite vertices of a unique face  $\Lambda$  in  $\mathcal{M}(\mathcal{S}, \mathcal{L})$ . This guarantees the existence of two edges  $e \in f$  and  $d \in g$  and two sequences of collapses  $e \rightarrow f_1, e_1 \rightarrow f_2, \dots, e_{k-1} \rightarrow f_k$  and  $d \rightarrow g_1, d_1 \rightarrow g_2, \dots, d_{k-1} \rightarrow g_l$ , where the edges  $e$  and  $d$  belongs to  $f$  and  $g$ , respectively, and both  $f_k$  and  $g_l$  contain the edge  $a$ . The uniqueness of the adjacency between  $a$  and  $f$  in  $\overline{\mathcal{S}}$  implies that reversing the sequence of collapses  $e \rightarrow f_1, e_1 \rightarrow f_2, \dots, e_{k-1} \rightarrow f_k$  does not create alternated closed

paths in the Morse matching. Let  $a \rightarrow f_k, e_{k-1} \rightarrow f_{k-1}, \dots, e_1 \rightarrow f_1, e \rightarrow f$  be this reversed sequence. Then the set

$$\{d \rightarrow g_1, d_1 \rightarrow g_2, \dots, d_{k-1} \rightarrow g_l, a \rightarrow f_k, e_{k-1} \rightarrow f_{k-1}, \dots, e_1 \rightarrow f_1, e \rightarrow f\}$$

is a Morse matching on  $\mathcal{S}$ , and Theorem A.1 provides the desired result. ■

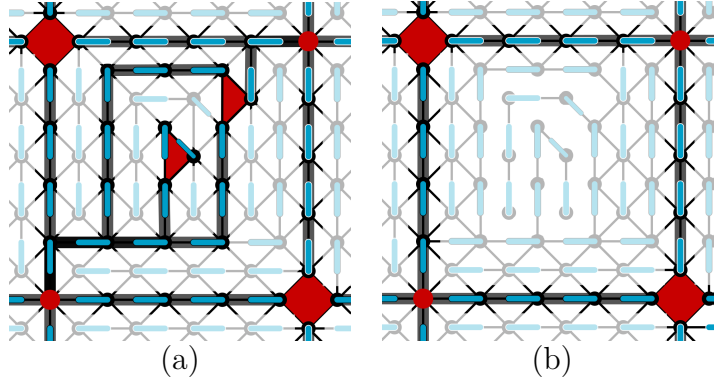


Figure 4.12: (a) the two critical triangles in red are in the boundary of a unique face of the MS decomposition. (b) the cancellation between the critical faces.

We now present a cancellation criterion between a vertex  $v$  and a face  $f$  in a discrete line field  $(\mathcal{S}, \mathcal{L})$ ; it is based on Forman's cancellation of critical elements in a Morse matching [23]. A path  $v = v_1 v_2 \dots v_k$  from  $v$  to a vertex  $v_k$  in the boundary walk of  $f$  can be reversed as follows. For each  $1 \leq i < k$  there is an edge  $e_i$  which runs from  $v_i$  to  $v_{i+1}$ , satisfying  $\{v_i, e_i\} \in \mathcal{L}$ . To reverse the path, consider  $\{v_i, e_i\} \in \mathcal{M}(\mathcal{S})$  and  $\{v_{i+1}, e_i\} \in \mathcal{L}$ , and  $\{v, e\} \in M$ , where  $e$  is a diagonal of  $f$ .

**Proposition 4.11** *Let  $v$  be a critical vertex and  $f$  a critical face, with  $\text{index}(f) < 0$ , connected by a unique path  $\gamma$ . One can reverse  $\gamma$  such that  $f$  is subdivided into two faces  $f_0 \cup e \cup f_1$  and the resulting vector field has  $v$  and  $f_0$  as non-critical cells satisfying  $\text{index}(f_1) = \text{index}(f) + \text{index}(v)$ .*

**Proof.** The reversion of the path  $\gamma$  does not create a cycle, since otherwise there would be another path between  $v$  and  $f$ , contradicting the proposition hypothesis; Figures 4.13(a) and (b) provide the proof idea. ■

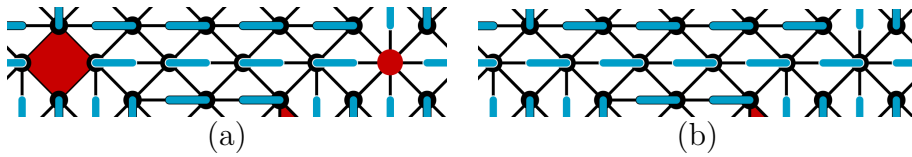


Figure 4.13: (a) a critical face and a critical vertex connected by a unique path. (b) the reversed path.

## 5

### From discrete line to discrete vector fields

In this chapter we give correspondence between discrete line fields and discrete vector fields, which motivates the use of discrete vector field constructions and analysis [29, 37, 38, 39, 40, 41, 42, 43] to study discrete line fields.

#### 5.1

##### Discrete vector fields and discrete line fields

The strategy used to build the correspondence between discrete vector fields and discrete line fields is based on considering two classes of discrete line fields: the orientable and the non-orientable fields. We prove that a subdivision of the critical faces of an orientable discrete line field produces a discrete vector field. For a non-orientable discrete line field, we suspend the field to an orientable line field, using the construction of branched coverings of surface decompositions proposed by Gross and Tucker [32].

##### 5.1.1

###### Orientable discrete line fields

Let  $(\mathcal{S}, \mathcal{L})$  be a discrete line field and  $\overline{\mathcal{S}} = (\overline{V}, \overline{E}, \overline{F})$  be the simple decomposition given by Theorem 4.8 applied to  $(\mathcal{S}, \mathcal{L})$ . The field  $(\mathcal{S}, \mathcal{L})$  is said to be *orientable* if the graph  $\overline{G} = (\overline{V}, \overline{E})$  is bipartite, and *non-orientable* otherwise (Figure 5.1).

Next we write the property of orientability of a discrete line field  $(\mathcal{S}, \mathcal{L})$  in terms of its unmatched edges. The set  $E(\mathcal{L})$  denotes the matched edges.

**Lemma 5.1** *Let  $(\mathcal{S}, \mathcal{L})$  be an orientable discrete line field. Then the graph  $(V, E - E(\mathcal{L}))$  is bipartite.*

**Proof.** By hypothesis,  $(\overline{V}, \overline{E})$  admits a bipartition  $\overline{W} \sqcup \overline{B}$ . We construct a bipartition  $W \sqcup B$  of  $(V, E - E(\mathcal{L}))$  as follows: a vertex  $v$  in  $V$  belongs to  $W$  if there is a path connecting  $v$  to a critical vertex in  $\overline{W}$ ; analogously for  $B$ . To verify that  $W \sqcup B$  is indeed a bipartition of  $(V, E - E(\mathcal{L}))$ , consider an edge  $e$  in  $E - E(\mathcal{L})$ . Then the endpoints of  $e$  are in different sets of the partition  $W \sqcup B$ , otherwise the critical vertices, connected to them by paths, must be adjacent in  $(\overline{V}, \overline{E})$ , contradicting its bipartition  $\overline{W} \sqcup \overline{B}$ . ■



From Lemma 5.1, the boundary walk of a face in an orientable discrete line field has an even number of unmatched edges (the reciprocal is false, Figure 5.1(a) provides a counterexample). We propose a face subdivision of the underlying decomposition that converts the orientable discrete line field into a discrete vector field.

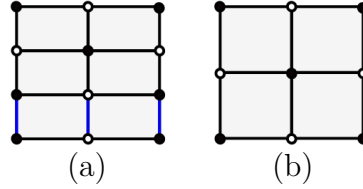


Figure 5.1: (a) and (b) present a non-bipartite 4-decomposition of the torus and a bipartite 4-decomposition.

**Lemma 5.2 (Face subdivision)** *Let  $f$  be a face with  $k > 2$  edges in its boundary walk. If  $k = c(f) > 4$  then  $f$  can be subdivided into one 4-gon and a  $(k - 2)$ -gon. If  $k \neq c(f)$  then  $f$  can be subdivided into a triangle with just one matched edge and a  $c(f)$ -gon.*

**Proof.** First, let  $k = c(f)$ , then  $f$  has no matched edges on its boundary walk. The number  $k$  is even by Lemma 5.1, and greater than 4, since  $k > 2$  by hypothesis. Let  $v_1e_1v_2e_2 \cdots v_ke_kv_1$  be the boundary walk of  $f$ . As  $k \geq 4$ , we can subdivide  $f$  into two faces,  $f_1$  and  $f_2$ , by adding an edge  $e$  joining the vertices  $v_1$  and  $v_4$ . The boundary walk of  $f_1$  and  $f_2$  are given by  $v_1e_1v_2e_2v_3e_3v_4ev_1$  and  $v_1ev_4e_4v_5e_5 \cdots v_ke_kv_1$ , respectively. Then,  $f_1$  is a 4-gon, and  $f_2$  is a  $(k - 2)$ -gon (Figures 5.2(a) and (b)).

When  $k \neq c(f)$ , we consider an unmatched edge  $e_1$  adjacent to a matched edge  $e_2$ . Such a configuration is allowed, since otherwise  $c(f) = 0$ , so by Theorem 4.8, the decomposition  $\overline{\mathcal{S}}$  is a sphere consisting only of a vertex and a face. Let  $v_1e_1v_2e_2v_3 \cdots v_ke_kv_1$  be the boundary walk of  $f$ . We can subdivide  $f$  into two faces,  $f_1$  and  $f_2$ , by adding an edge  $e$  joining the vertices  $v_1$  and  $v_3$ . The boundary walk of  $f_1$  and  $f_2$  are given by  $v_1e_1v_2e_2v_3ev_1$  and  $v_1ev_3e_3v_4e_4 \cdots v_ke_kv_1$ , respectively. Then,  $f_1$  is a triangle with just one matched edge  $e_2$ , and  $f_2$  is a  $c(f)$ -gon (Figures 5.2(c) and (d)). ■

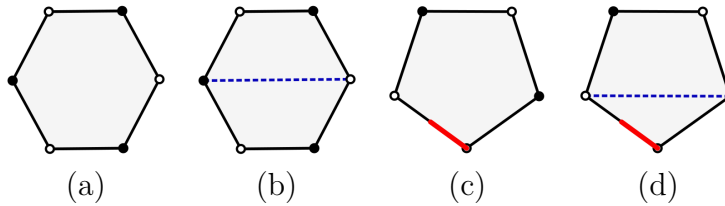


Figure 5.2: (a) a hexagon with no matched edge; in (b) a subdivision into two 4-gons. (c) a pentagon with a unique matched edge; (d) a subdivision into a 4-gon and a regular triangle.

Applying Lemma 5.2 inductively on an orientable discrete line field, we obtain a discrete vector field.

**Theorem 5.3** *Let  $(\mathcal{S}, \mathcal{L})$  be an orientable discrete line field. There is a subdivision of faces of  $\mathcal{S}$  producing a discrete vector field  $(\mathcal{S}', \mathcal{L})$ .*

**Proof.** The application of Lemmas 5.2 and 4.6, inductively, on the faces of  $(\mathcal{S}, \mathcal{L})$  produces a discrete line field  $(\mathcal{S}', \mathcal{L})$  with only regular triangles and critical 4-gons without matched edges. In other words, a discrete vector field is obtained. ■

### 5.1.2

#### Non-orientable discrete line fields: double branched coverings

For non-orientable discrete line fields, that is, when the graph of unmatched edges is not bipartite, we use a double branched covering defined below, which suspends the field to an orientable discrete line field.

We will use the same definitions by Gross and Tucker from [32]. Let  $\mathbb{Z}_2$  be the cyclic group of order two,  $G = (V, E)$  a graph and  $\alpha : E \rightarrow \mathbb{Z}_2$  be a function over its set of edges  $E$ . The *derived graph*  $\tilde{G}$  of the pair  $(G, \alpha)$  is defined by considering its vertex set being  $\tilde{V} = V(G) \times \mathbb{Z}_2$  and edge set  $\tilde{E} = E(G) \times \mathbb{Z}_2$ , such that for each edge  $e = [u, v] \in E$  we define  $e \times i = [u \times i, v \times (i + \alpha(e))]$  for  $i = 0, 1$  (Figure 5.3).

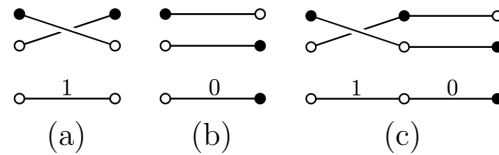


Figure 5.3: Different colors receive the number 0, and 1 otherwise. (a) the suspension of an edge signed with 1. (b) the suspension of an edge signed with 0. (c) combines (a) and (b).

The natural projection  $p : \tilde{G} \rightarrow G$  is a double covering map since the edges of  $G$  have two copies in  $\tilde{G}$  and the degree of each vertex is preserved by the construction of  $\tilde{G}$  (Figure 5.3(c)). We show that a rotational system can be suspended. Let  $\mathcal{R}$  be a rotational system over  $G$ . One can define a *derived suspension*  $\tilde{\mathcal{R}}$ : For the rotation  $e_1, e_2, \dots, e_k$  on each vertex  $v$  of  $G$  lifted to  $v \times i$  on the derived graph  $\tilde{G}$ , consider the rotation  $e_1 \times i, e_2 \times i, \dots, e_k \times i$ . Theorem 2.1, in turn, provides the *derived surface*  $\tilde{S}$ , in which the derived graph  $\tilde{G}$  is embedded.

Gross and Tucker [32] proved that the map  $p : \tilde{G} \rightarrow G$  induces a branched covering between  $\tilde{S}$  and  $S$  (Figure 5.4).

**Theorem 5.4 (Gross–Tucker [32])** *Let  $\mathcal{S} = (V, E, F)$  be a decomposition of an oriented compact surface  $S$  and  $\alpha : E \rightarrow \mathbb{Z}_2$  a function. One can extend the covering map  $p : \tilde{G} \rightarrow G$  to a double branched covering  $p : \tilde{S} \rightarrow S$  between their embedding surfaces, such that: If  $\alpha(e_1) + \dots + \alpha(e_k) = 1$  on the boundary walk  $v_1 e_1 v_2 e_2 \dots v_k e_k v_1$  of a face  $f$  then the map  $p$  restricted to  $f$  consists of the complex map  $z^2$ . Otherwise the pre-image of  $f$  is two disjoint copies of  $f$ .*

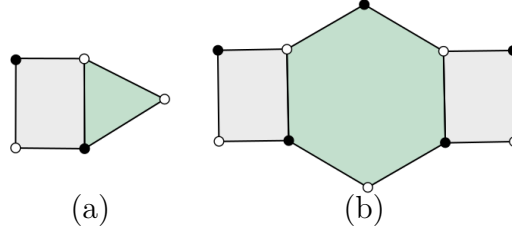


Figure 5.4: The edges assignment is similar to Figure 5.3. (a) a decomposition containing two faces; (b) the derived decomposition.

The embedding of the derived graph  $\tilde{G} = (\tilde{V}, \tilde{E})$  into the derived surface  $\tilde{S}$  provides the *derived decomposition*  $\tilde{\mathcal{S}} = (\tilde{V}, \tilde{E}, \tilde{F})$  of  $\tilde{S}$ .

Next we use Theorem 5.4 to suspend a non-orientable discrete line field to an oriented field on a derived decomposition.

Let  $\mathcal{S} = (V, E, F)$  be a decomposition of a compact connected orientable surface  $S$  and  $(\mathcal{S}, \mathcal{L})$  be a non-orientable discrete line field. Define a function  $\alpha : E \rightarrow \mathbb{Z}_2$  on the edges of  $G = (V, E)$ , such that  $\alpha(e) = 1$  if  $e$  is unmatched by  $\mathcal{L}$  and 0 otherwise. Then the derived graph  $\tilde{G} = (\tilde{V}, \tilde{E})$  covers  $G$  twice: suspend each matched pair of vertex-edge to two copies in  $\tilde{G}$ . The result is a matching  $\tilde{\mathcal{L}}$  between vertices and edges of the derived decomposition on  $\tilde{\mathcal{S}}$ , that is, a discrete line field  $(\tilde{\mathcal{S}}, \tilde{\mathcal{L}})$  (Figure 5.5).

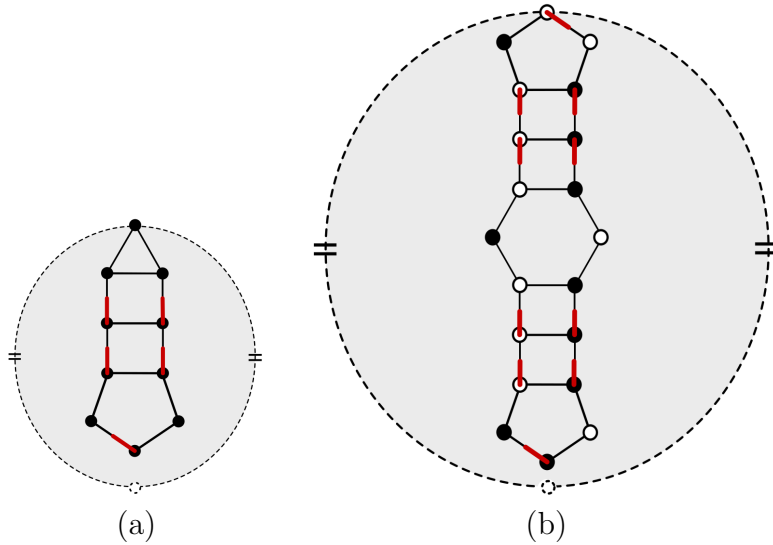


Figure 5.5: (a) a non-orientable discrete line field. (b) the suspension to an orientable field.

Using the properties given by Theorem 5.4 the next result follows.

**Theorem 5.5** *Let  $(\mathcal{S}, \mathcal{L})$  be a discrete line field. The discrete line field  $(\widetilde{\mathcal{S}}, \widetilde{\mathcal{L}})$  is orientable.*

The suspension  $(\widetilde{\mathcal{S}}, \widetilde{\mathcal{L}})$  of a discrete line field  $(\mathcal{S}, \mathcal{L})$  corresponds to a discrete vector field. Specifically,  $(\widetilde{\mathcal{S}}, \widetilde{\mathcal{L}})$  is an orientable discrete line field by Theorem 5.5, then Theorem 5.3 applied to this field provides through a subdivision the desired discrete vector field  $(\widetilde{\mathcal{S}}', \widetilde{\mathcal{L}})$ .

## 6

### Conclusion and future work

This thesis provided a combinatorial framework to approach line fields. The main object was the self-contained definition of discrete line fields that encoded Forman's construction for vector fields.

For computational issues, discrete line fields admit the following simple algorithmic constructions without any numerical parameters:

- The *critical point detection* is made through the formula  $\frac{c(f)}{2} - 1$  which is easily computed (linear time);
- The *connection between critical elements* is determined by the paths (linear time);
- The *MS decomposition* is essentially determined through a rotational system (linear time). The face each cell belongs to can be determined through a path and the rotational system (linear time);
- The *reduction of critical elements* is made by removing edges or reversing paths of the discrete line field (linear time).

The simplicity and combinatorial nature of the constructions above motivate their use in geometry processing applications. The main challenge in this context is to match the construction of a discrete line field with the geometry of a sampled surface, e.g. the principal curvature directions in Figure 6.1.

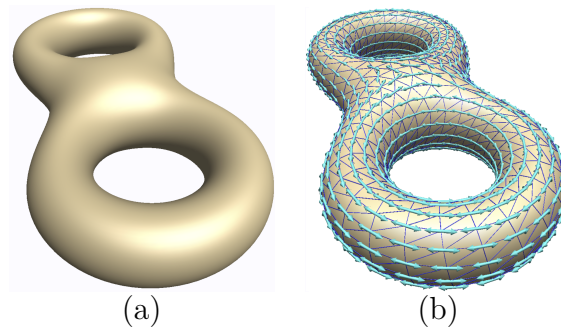


Figure 6.1: (a) a bitorus. (b) a sample of the minimum curvature vector field over the vertices of a decomposition of the bitorus.

We also provided a suspension of a discrete line field to a discrete vector field. Thus geometric constructions for discrete vector fields [39, 40, 43, 38, 42, 29] can be used to study discrete line fields.

The definitions and results behind discrete line fields motivate many questions. For instance:

- Can we consider cycles in the definition of discrete line fields?
- Is it possible to extend the definition of discrete line fields to higher dimensions?
- Is there any relation between discrete line fields and other discrete definitions for line fields (for example, the discrete version of line field presented in *discrete exterior calculus* [11])?

In a nutshell, we proposed a consistent combinatorial point of view for line fields, usually approached in computer graphics/geometry processing/discrete geometry through numerical methods. We hope that this technique can be explored and applied to new offer perspectives.

## Bibliography

- [1] HELMAN, J. L.; HESSELINK, L. Visualizing vector field topology in fluid flows, **IEEE Computer Graphics and Applications**, v.11, n.3, p. 36–46, 1991.
- [2] DELMARCELLE, T.; HESSELINK, L. Visualizing second-order tensor fields with hyperstreamlines, **IEEE Computer Graphics and Applications**, v.13, n.4, p. 25–33, 1993.
- [3] DONG, S.; BREMER, P.-T.; GARLAND, M.; PASCUCCI, V. ; HART, J. C. **Spectral surface quadrangulation**. In: *ACM Transactions on Graphics*, v. 25, p. 1057–1066. ACM, 2006.
- [4] HUANG, J.; ZHANG, M.; MA, J.; LIU, X.; KOBBELT, L. ; BAO, H. **Spectral quadrangulation with orientation and alignment control**. In: *ACM Transactions on Graphics*, v. 27, p. 147. ACM, 2008.
- [5] KÄLBERER, F.; NIESER, M. ; POLTHIER, K. **Quadcover-surface parameterization using branched coverings**. In: *Computer graphics forum*, v. 26, p. 375–384. Wiley Online Library, 2007.
- [6] ALLIEZ, P.; COHEN-STEINER, D.; DEVILLERS, O.; LÉVY, B. ; DESBRUN, M. Anisotropic polygonal remeshing, **ACM Trans. Graph.**, v.22, n.3, p. 485–493, 2003.
- [7] MARINOV, M.; KOBBELT, L. **A robust two-step procedure for quad-dominant remeshing**. In: *Computer Graphics Forum*, v. 25, p. 537–546. Wiley Online Library, 2006.
- [8] NASCIMENTO, R. **Cancelamento de Singularidades em Campos de Cruzes**. 2015. PhD thesis, PUC-Rio.
- [9] AUER, C.; HOTZ, I. **Complete tensor field topology on 2d triangulated manifolds embedded in 3d**. In: *Computer Graphics Forum*, v. 30, p. 831–840. Wiley Online Library, 2011.
- [10] DELMARCELLE, T.; HESSELINK, L. **The topology of symmetric, second-order tensor fields**. In: *Proceedings of the conference on Visualization'94*, p. 140–147. IEEE Computer Society Press, 1994.

- [11] KNÖPPEL, F.; CRANE, K.; PINKALL, U. ; SCHRÖDER, P. **Stripe patterns on surfaces**, *ACM Transactions on Graphics*, v.34, n.4, p. 39, 2015.
- [12] NASCIMENTO, R.; PAIXAO, J.; LOPES, H. ; LEWINER, T. **Topology aware vector field denoising**. In: *Graphics, Patterns and Images (SIBGRAPI)*, 2010 23rd SIBGRAPI Conference on, p. 103–109. IEEE, 2010.
- [13] SREEVALSAN-NAIR, J.; AUER, C.; HAMANN, B. ; HOTZ, I. **Eigenvector-based interpolation and segmentation of 2d tensor fields**. In: *Topological Methods in Data Analysis and Visualization*, p. 139–150. Springer, 2011.
- [14] TRICOCHE, X. **Vector and tensor field topology simplification, tracking, and visualization**. 2002. PhD thesis, Schriftenreihe Fachbereich Informatik (3), Universität.
- [15] WANG, B.; HOTZ, I. **Robustness for 2d symmetric tensor field topology**. In: *Modeling, Analysis, and Visualization of Anisotropy*, p. 3–27. Springer, 2017.
- [16] BRONSHTEYN, I.; NIKOLAEV, I. **Peixoto graphs of Morse-Smale foliations on surfaces**, *Topology and its Applications*, v.77, n.1, p. 19–36, 1997.
- [17] PEIXOTO, M. M. **On the classification of flows on two manifolds**, *Proc. Sympos. Univ. of Bahia, Salvador, Brazil*, 1971, v.77, n.1, p. 389–419, 1973.
- [18] SPIVAK, M. **A Comprehensive Introduction to Differential Geometry**, v. 3. Publish or Perish, INC, 1999.
- [19] ANDRONOV, A.; PONTRYAGIN, L. **Rough systems**, *DAN*, v.14, n.5, p. 247–250, 1937.
- [20] NIKOLAEV, I. **Foliations on surfaces**, v. 41. Springer, 2013.
- [21] MORSE, M. **Bowls of a non-degenerate function on a compact differentiable manifold**. In: *Differential and Combinatorial Topology (A Symposium in Honor of Marston Morse)*, p. 81–103. Princeton University Press, 1965.
- [22] FORMAN, R. **Combinatorial vector fields and dynamical systems**, *Mathematische Zeitschrift*, v.228, n.4, p. 629–681, 1998.



- [23] FORMAN, R. Morse theory for cell complexes, **Advances in Mathematics**, v.134, n.1, p. 90–145, 1998.
- [24] BRONSHTEYN, I.; NIKOLAEV, I. Structurally stable fields of line elements on surfaces, **Nonlinear Analysis: Theory, Methods & Applications**, v.34, n.3, p. 461–477, 1998.
- [25] NIKOLAEV, I. Graphs and flows on surfaces, **Ergodic Theory and Dynamical Systems**, v.18, n.1, p. 207–220, 1998.
- [26] ARCHDEACON, D. The medial graph and voltage-current duality, **Discrete mathematics**, v.104, n.2, p. 111–141, 1992.
- [27] NEDELA, R.; ŠKOVIERA, M. Remarks on diagonalizable embeddings of graphs, **Mathematica Slovaca**, v.40, n.1, p. 15–20, 1990.
- [28] PISANSKI, T.; MALNIC, A. **The diagonal construction and graph embeddings**. In: Proceedings of the Fourth Yugoslav Seminar on Graph Theory, p. 271–290, 1983.
- [29] REININGHAUS, J.; HOTZ, I. Combinatorial 2d vector field topology extraction and simplification, **Topological Methods in Data Analysis and Visualization**, p. 103–114, 2011.
- [30] WEINKAUF, T.; GINGOLD, Y. ; SORKINE, O. **Topology-based smoothing of 2d scalar fields with C1-continuity**. In: Computer Graphics Forum, v. 29, p. 1221–1230. Wiley Online Library, 2010.
- [31] WEINKAUF, T.; THEISEL, H.; SHI, K.; HEGE, H.-C. ; SEIDEL, H.-P. **Extracting higher order critical points and topological simplification of 3d vector fields**. In: Visualization, 2005. VIS 05. IEEE, p. 559–566. IEEE, 2005.
- [32] GROSS, J. L.; TUCKER, T. W. **Topological graph theory**. Wiley, 1987.
- [33] STAHL, S. Generalized embedding schemes, **Journal of Graph Theory**, v.2, n.1, p. 41–52, 1978.
- [34] TRICOCHÉ, X.; SCHEUERMANN, G.; HAGEN, H. ; CLAUSS, S. **Vector and tensor field topology simplification on irregular grids**. In: VisSym, v. 1, p. 107–116, 2001.
- [35] PEIXOTO, M. M. Structural stability on two-dimensional manifolds, **Topology**, v.1, p. 101–120, 1962.

- [36] MILNOR, J. **Morse theory**. Princeton university press, 1963.
- [37] ADIPRASITO, K.; BENEDETTI, B. **Metric geometry and collapsibility**. Citeseer, 2011. Technical report.
- [38] GYULASSY, A. G. **Combinatorial construction of Morse-Smale complexes for data analysis and visualization**. 2008. PhD thesis, University of California, Davis.
- [39] LEWINER, T.; LOPES, H. ; TAVARES, G. Optimal discrete Morse functions for 2-manifolds, **Computational Geometry**, v.26, n.3, p. 221–233, 2003.
- [40] PAIXÃO, J. **Analysis of Morse matchings: parameterized complexity and stable matching**. 2014. PhD thesis, PUC-Rio.
- [41] PAIXAO, J.; LAGOAS, J.; LEWINER, T. ; NOVELLO, T. Greedy Morse matchings and discrete smoothness, **arXiv**, v.abs/1801.10118, 2018.
- [42] REININGHAUS, J. **Computational discrete Morse theory**. 2012. PhD thesis, Freie Universität Berlin.
- [43] ROBINS, V.; WOOD, P. J. ; SHEPPARD, A. P. Theory and algorithms for constructing discrete Morse complexes from grayscale digital images, **IEEE Transactions on pattern analysis and machine intelligence**, v.33, n.8, p. 1646–1658, 2011.
- [44] PLACHTA, L. The combinatorics of gradient-like flows and foliations on closed surfaces: I. topological classification, **Topology and its Applications**, v.128, n.1, p. 63–91, 2003.
- [45] LEWINER, T.; NOVELLO, T.; PAIXAO, J. ; TOMEI, C. Discrete gradient line fields on surfaces, **arXiv**, v.abs/1712.08136, 2017.
- [46] CHARI, M. K. On discrete Morse functions and combinatorial decompositions, **Discrete Mathematics**, v.217, n.1-3, p. 101–113, 2000.

## PUC-Rio - Certificação Digital Nº 1412645/CA

A *matching* in  $\mathcal{H}(\mathcal{S})$  is a collection  $\mathcal{X}$  of disjoint edges in the Hasse diagram  $\mathcal{H}(\mathcal{S})$ . Clearly  $\mathcal{X}$  is the disjoint union of the sets of edges  $\mathcal{X}_V$  and  $\mathcal{X}_F$  containing elements in  $V$  and  $F$ , respectively. Following the notation from Forman [23] and Chari [46], a *Morse matching* is a matching in  $\mathcal{H}(\mathcal{S})$  for which neither  $\mathcal{X}_V$  nor  $\mathcal{X}_F$  contains a set of alternating edges of a closed cycle of  $\mathcal{H}(\mathcal{S})$ . Figure A.1(c) provides a Morse matching.



**Theorem A.1 (Forman [23])** *Any decomposition  $\mathcal{S}$  of  $S$  endowed with a Morse matching  $\mathcal{X}$  over its Hasse diagram is homotopy equivalent to a decomposition  $\overline{\mathcal{S}}$ , whose  $p$ -cells are the critical  $p$ -cells.*

In classical Morse theory [36], the negative of a Morse function is a Morse function. The discrete version of this result was also presented by Forman [23], and it consists of dualizing both the underlying decomposition and its pairing of cells. More precisely, let  $\mathcal{S}$  be a decomposition of a compact surface  $S$ , and  $\mathcal{X}$  be a Morse matching on the Hasse diagram  $\mathcal{H}(\mathcal{S})$ . As  $\mathcal{H}(\mathcal{S})$  is isomorphic to

the Hasse diagram  $\mathcal{H}(\mathcal{S}^*)$  of the dual composition  $\mathcal{S}^*$  of  $\mathcal{S}$  (folkloric result), the Morse matching  $\mathcal{X}$  corresponds to Morse matching in  $\mathcal{H}(\mathcal{S}^*)$ . This is called the *dual* Morse matching of  $\mathcal{X}$  and denoted by  $\mathcal{X}^*$ .

Following the notation of the previous paragraph, Theorem A.1 applied to both  $\mathcal{X}$  and to its negative  $\mathcal{X}^*$  produces dual decompositions of the surface  $S$  [23]. Then, their Hasse diagrams are isomorphic, producing equivalent decompositions of the surface  $S$ .